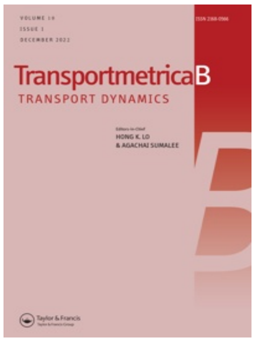

Transportmetrica B: Transport Dynamics

ISSN: 2168-0566 (Print) 2168-0582 (Online) Journal homepage: www.tandfonline.com/journals/ttrb20

How is commute mode choice related to 2D and 3D land use mix? a case study of central Suqian City

Yi Zhu, Xiao Qin, Ruotong Wu & Feng Zhen

To cite this article: Yi Zhu, Xiao Qin, Ruotong Wu & Feng Zhen (2026) How is commute mode choice related to 2D and 3D land use mix? a case study of central Suqian City, Transportmetrica B: Transport Dynamics, 14:1, 2622498, DOI: 10.1080/21680566.2026.2622498

To link to this article: https://doi.org/10.1080/21680566.2026.2622498

Published online: 29 Jan 2026.

TRANSPORTMETRICA B: TRANSPORT DYNAMICS
2026, VOL. 14, NO. 1, 2622498
https://doi.org/10.1080/21680566.2026.2622498

Taylor & Francis
Taylor & Francis Group

RESEARCH ARTICLE

How is commute mode choice related to 2D and 3D land use mix? a case study of central Suqian City

Yi Zhu[a], Xiao Qin[a,b], Ruotong Wu[a] and Feng Zhen[a,b]

[a]School of Architecture and Urban Planning, Nanjing University, Nanjing, People's Republic of China; [b]Key Laboratory of Urban AI and Green Built Environment of Provincial Higher Education Institutes, Nanjing University, Nanjing, People's Republic of China

ABSTRACT

Understanding residents' commute mode choice and its influencing factors is crucial for alleviating traffic congestion. Current research on land use mix has largely focused on 2D space, with limited attention to how 2D and 3D land use mix and their threshold effects differentially influence residents' commuting behavior. To address this gap, this study empirically examines Suqian, a prefecture-level city in China, by deriving land use mix characteristics from land use, building, and POI data. Then applied the XGBoost model to test and compare the nonlinear impacts of land use mix features on the mode shares of different commute modes. The results indicate that the importance and threshold effects of 2D and 3D land use mix variables differ across commute mode choices, thereby identifying their effective ranges. The study theoretically enriches the land-use and transport interaction framework and practically provides references for land use policies to alleviate traffic congestion.

ARTICLE HISTORY
Received 28 September 2025
Accepted 20 January 2026

KEYWORDS
2D and 3D land use mix; commute mode choice; machine learning; traffic congestion management

1 Introduction

In the mid-to-late 20th century, suburban sprawl in Western cities led to energy waste and urban decay, drawing attention to land use mix as a remedy for car-dependent urban forms (Grant 2002). In contrast, China has followed a different path of urban development, characterised by rapid urbanisation and high-density built environments, where land use mix is viewed as a strategy to optimise spatial efficiency rather than to counter suburban sprawl. As urban renewal movements grew in the U.S. and Europe, land use mix became a key strategy to boost urban vitality and reduce commuting pressures (Jacobs 1993; Kong et al. 2015). Since the onset of rapid urbanisation in China, the massive concentration of urban population and the growing but still transitional motorisation have led to increasing traffic pressure, making residents' commute mode choice particularly critical in this context. These changes highlight the impact of land use mix on commute mode choice. Commute mode choice not only affects the operational efficiency of urban transport systems and helps alleviate traffic congestion, but also enhances residents' quality of life and reduces carbon emissions (Yang et al. 2018; De Vos et al. 2021; Zhu et al. 2023; Zou et al. 2025; Xia et al. 2025). UN-Habitat points out that urban planning should encourage mixed land use to enhance functional complementarity and accessibility, thereby exerting positive effects on traffic pressure and commuting demand (UN-Habitat 2013). The Chinese government has emphasised revitalising inefficient land stock and promoting mixed land development (Agency 2025). Moreover, while empirical evidence from cities such as Los Angeles demonstrates that density, land use mix, and connectivity influence travel behaviour, in China, the same principles are applied within a high-density, transit-oriented, and redevelopment-driven context. This points to a universally shared consensus that compact, mixed land use advances sustainable mobility, though this consensus is embedded in diverse urban realities (Litman 2017).

Traditional studies on land use mix have mainly focused on two-dimensional (2D) space (Song, Merlin, and Rodriguez 2013; Tian, Liang, and Zhang 2017; Zhuo et al. 2019). Although many recent studies have adopted Points of Interest (POI) data to describe functional diversity, such methods typically rely on the planar distribution of POI coordinates. Even when multiple POIs exist within the same building, they are usually

CONTACT Xiao Qin x.qin@nju.edu.cn School of Architecture and Urban Planning, Nanjing University, 210093, Room 809, Jianliang Building, No. 22, Hankou Road, Nanjing, People's Republic of China

projected onto the same horizontal surface, without accounting for attributes such as floor level or building volume. As a result, these approaches essentially remain within a two-dimensional analytical framework. With the emergence of high-density and vertical urban development, reliance on purely 2D indicators tends to underestimate the significance of high-rise multifunctional buildings, while simultaneously overestimating the influence of extensive low-rise land uses (Zhao, Xia, and Li 2023), this may lead to a mismatch between land use and transport supply and demand, potentially resulting in a disconnect between transit routes, public facility provision, and actual needs. In recent years, the advancement of spatial data acquisition technologies, such as street view imagery and building information modelling (BIM), has enabled the accurate measurement of three-dimensional (3D) land use characteristics. The incorporation of 3D indicators not only captures the vertical layering of different functions but also reflects the growing complexity and intensity of urban space (Kalogianni et al. 2020). Integrating 2D and 3D indicators to reconstruct the measurement of land use mix can overcome the limitations of planar analysis (An et al. 2025).

This study takes Suqian City, China as a case and integrates POI data, building data, and mobile signalling data. It maintains the generality and comparability of 2D indicators while simultaneously employing 3D indicators to address the limitations of 2D measures, such as the tendency to underestimate the impact of high-rise multifunctional buildings. In this way, it provides a more comprehensive and accurate depiction of land use mix. Combined with commuting mode choice data obtained from questionnaire surveys, the study applies the XGBoost model and the SHAP interpretability framework to systematically examine the impacts of 2D and 3D land use mix on residents' commuting mode choice. In this context, addressing these gaps by incorporating a three-dimensional perspective into the land use mix framework can enrich the theoretical understanding of built environment–commuting interactions, particularly in capturing nonlinear mechanisms and spatial heterogeneity. Theoretically, this approach advances the transition from a conventional 2D planning paradigm to a more integrated 2D and 3D framework. Practically, as Suqian represents a medium-sized city, this study provides valuable implications for formulating land use mix strategies to mitigate traffic congestion in similar urban contexts. Figure 1 illustrates the technical framework of this study.

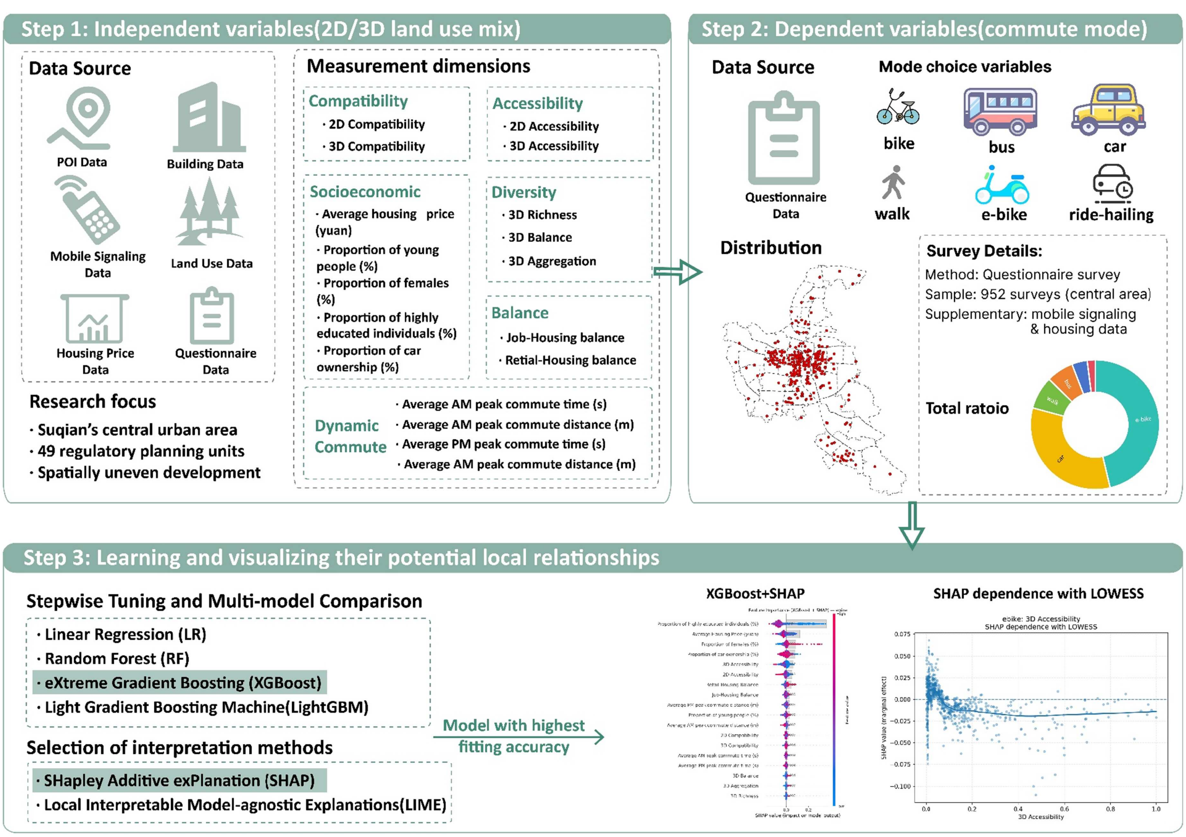

Figure 1. Research framework.

2 Literature review

2.1 Land use mix and commute mode choice

Traditional commute modes include private cars, public transit, e-bike, cycling, and walking. With improvements in living standards and technological advancement, new options such as ride-hailing have become increasingly prevalent. Existing studies have identified several key determinants of commuting mode choice, including built environment attributes such as density, land-use mix, and proximity to transit hubs, as well as car ownership and individual attitudes toward different transport options (Sun, Ermagun, and Dan 2017; Wang et al. 2020; Ashik et al. 2024; Hawkins and Nurul Habib 2024; Chen et al. 2025; Guo et al. 2025). From a broader perspective, the interaction between transportation systems and land use is widely recognised as a key mechanism shaping travel behaviour and urban spatial structure. Specifically, transport infrastructure, especially major transit corridors, simultaneously reflects and reconfigures land development, functional diversity, and commuting dynamics (Zhang et al. 2025). Both objective and perceived features of the built environment have been found to influence mode choice directly or indirectly, often mediated by factors such as car ownership and commuting distance (Rith, Alexis, and Biona 2019). It is important to note that most of these studies have primarily focused on the relationship between two-dimensional (2D) land use mix and commuting patterns, commonly operationalized through diversity, accessibility, and compatibility indices. However, this 2D perspective remains limited in high-density urban contexts and may not fully capture the multidimensional impacts of land use on commuting behaviour.

Studies have shown that long commuting distances, car ownership, high income, and low parking costs encourage car commuting, while high-quality transit services, TOD models, and high-density mixed land use promote public transport (Ma et al. 2018; Nourinejad and Amirgholy 2022). Moderate commuting distances, well-connected road networks, and land use mix support cycling, whereas very short distances, walkable streets, and good air quality foster walking (Wang et al. 2021; Chen et al. 2023; Jian et al. 2023; Zhang et al. 2025; Wei et al. 2025). Overall, the literature has evolved from traditional 2D indicators to 3D perspectives, and the integration of big data and advanced methods has deepened the understanding of land use–commuting relationships. However, most studies have focused on megacities, with relatively limited attention given to the characteristics of small- and medium-sized cities. Table 1 summarises existing studies on the relationship between land use and commuting characteristics, outlining their research focus, study areas, applied methods, and sources.

2.2 2D and 3D land use mix: concept and measurement

With the increasing utilisation of vertical urban space, indices based solely on two-dimensional geographic data can hardly capture the actual conditions in three-dimensional space (Wu, Lung, and Jan 2013; Manaugh and Kreider 2013; Babahajiani et al. 2017). In practice, certain land use types, such as residential and commercial, occupy relatively small surface areas but have large building volumes and multiple floors, involving intensive socio-economic activities. Measuring land use mix solely by land area underestimates

Table 1. Relevant Research on Land and Commuting Patterns.

Study focus	Study area	Methodology	Key Authors/ Sources
Examined how land use mix and density affect commuting mode choice and car ownership	U.S. metropolitan areas (Household Travel Survey 1985)	Linear regression	(Cervero 1996)
Investigated the role of the "5Ds" (density, diversity, design, destination accessibility, distance to transit) in mode choice in a high-density city	Hong Kong	Multiple regression analysis	(Lu et al. 2018)
Explored how the built environment influences commuting distance	Beijing, China	Gradient Boosting Decision Trees (GBDT)	(Shen et al. 2023)
Assess the impact of residential–employment mix on commuting response ratio	Wuhan, China	Structural Equation Modelling (SEM)	(Zhou et al. 2022)
Analyse built environment influences on commuting mode choice	Megacity context (unspecified)	LightGBM/Random Forest	(Ashik et al. 2024)
Compared 2D and 3D built environment indicators, showing stronger effects of 3D measures on commuting-related carbon emissions	Urban case study (unspecified)	Spatial Durbin Model (SDM)	(Xia et al. 2025)

their influence. Conversely, land uses with large surface areas but relatively small building volumes, such as industrial land, tend to be overestimated in two-dimensional measures (Evans, Liddiard, and Steadman 2019). Therefore, it is necessary to optimise and reconstruct the methodology for calculating three-dimensional land use mix indices. For example, the FLUS-3D model to simulate future land use dynamics in vertical dimensions (Xu, Ding, and Liu 2024). While current Chinese planning policies, such as the "multi-plan integration" reform (Ministry of Natural Resources of the People's Republic of China 2025), do not explicitly address 3D land use mix, they create an institutional basis for future inclusion (State Council of the People's Republic of China 2025). In addition, some recent studies have employed POI data to describe the functional mix of urban spaces. While POI data can partially reflect the internal functional diversity of buildings, since multiple POIs may exist within a single structure, they are still typically analysed based on planar coordinates without floor-level or volumetric information. Therefore, such applications remain within a two-dimensional analytical framework rather than a true representation of vertical spatial complexity. In summary, the incorporation of 3D mix indices helps bridge the gap between theory and practice, significantly enriching the research framework of land use mix and enhancing the systematisation and precision of urban planning (An et al. 2025).

The measurement of land use mix typically considers multiple dimensions. Zhao, Xia, and Li (2023) pointed out that existing studies mainly measure land use mix from three dimensions: diversity, accessibility, and compatibility. Diversity, measured by entropy indices, reflects the number and balance of land uses and correlates with travel distance and vehicle use (Song, Merlin, and Rodriguez 2013). Accessibility captures the ease of reaching opportunities and is often the strongest built-environment factor, commonly assessed with gravity or cumulative-opportunity methods (Dovey and Pafka 2017). Compatibility evaluates synergies or conflicts among adjacent uses, such as residential–commercial complementarity or residential–industrial tension, with indices like compatibility mix degree (Manaugh and Kreider 2013). Balance emphasises functional equilibrium: jobs–housing balance reduces commuting distance, while retail–housing balance supports walking and short trips (Zhang and Zhao 2017). Socioeconomic attributes such as gender, age, education, further shape mode choice. Yet existing studies largely overlook dynamic commuting features. Evidence shows that congestion, reliability, and travel time during peak hours significantly alter travel behaviour, highlighting the need to integrate dynamic indicators for a more accurate assessment of land use mix (Zhang et al. 2025).

2.3 Models used in related studies

Methodologically, previous studies have used traditional statistical models (such as OLS, global spatial models, GWR) to explore the relationship between the built environment and commute mode choice (Gutiérrez, Cardozo, and García-Palomares 2011; Cardozo et al. 2012; Cui, Mishra, and Welch 2014; Sun and Yin 2019), but linear regression only captures global homogeneous relationships, leading to overfitting. On the one hand, built environment factors may only have a significant impact on commuting behaviour once they reach a certain level; otherwise, their effects may be underestimated. On the other hand, the influence of these factors may plateau or diminish beyond a certain threshold (Yang et al. 2021; Ao et al. 2025).Recent studies have introduced machine learning models, such as GBDT, XGBoost and LightGBM, to better capture complex nonlinear relationships and spatial heterogeneity (van Wee and Handy 2016; Ding, Cao, and Næss 2018; Alagbé et al. 2023). The application of interpretability methods such as SHAP and LIME (Lee et al. 2023), also supported the visualisation and threshold identification of the built environment–commuting mechanism (Ma et al. 2022; Zhang et al. 2025). Research indicates that land use mix can enhance urban vitality and reduce commuting time to some extent. However, excessive land use mix may lead to diminishing marginal returns (Raux, Lamatkhanova, and Grassot 2021). Therefore, it is necessary to investigate the nonlinear effects and threshold dynamics of land use mix elements across different commute mode choices.

3 Study area and data processing

3.1 Study area

This study focuses on the central urban area of Suqian, a prefecture-level city in Jiangsu Province, China, which was designated as such in 1996. The central urban area covers approximately 664.09 square kilometres, with a population of around 1.63 million and an urbanisation rate of about 65%, and includes 49 regulatory planning units. Suqian, a medium-sized prefecture-level city in eastern China, represents both the particularities of Chinese urbanisation and conditions shared by many global cities. On the one hand, its planning and development patterns reflect China's unique institutional and socio-economic context; on the other, its rapid urban growth, increasing vehicle ownership, and demand for mixed-use development resonate with the broader issues faced by other developing countries. Selecting Suqian as a case study thus not only highlights the significance of optimising land use mix in China but also provides valuable lessons for cities across the Global South that are experiencing or will soon experience similar urbanisation pressures. Figure 2 shows the geographical location of the study area and the distribution frequencies of various commuting modes.

3.2 Data resource

Based on Suqian City's mobile signalling data, the study divides the area using community detection algorithms, with traffic zones as the basic unit of analysis. We collected mobile signalling data, POI data, land use data and building data to measure land use mix. Mobile signalling data and field survey data were introduced to identify commuting behaviour. For analytical simplicity, land use categories were consolidated into six types: Business, Industry, Office, Other, Public Service, and Residence. The data sources are as follows and are summarised in Table 2.

The commuting data used in this study were obtained from a questionnaire survey conducted in the central urban area of Suqian in 2025. The survey collected information on residents' socio-economic attributes, commuting modes, travel time, and trip distance. A total of 952 valid responses were obtained and aggregated into 147 traffic analysis zones (TAZs). These TAZs were delineated from the original 49 regulatory planning units using mobile signalling data and refined through a community detection algorithm to better capture actual commuting communities. This spatial delineation enables a finer-

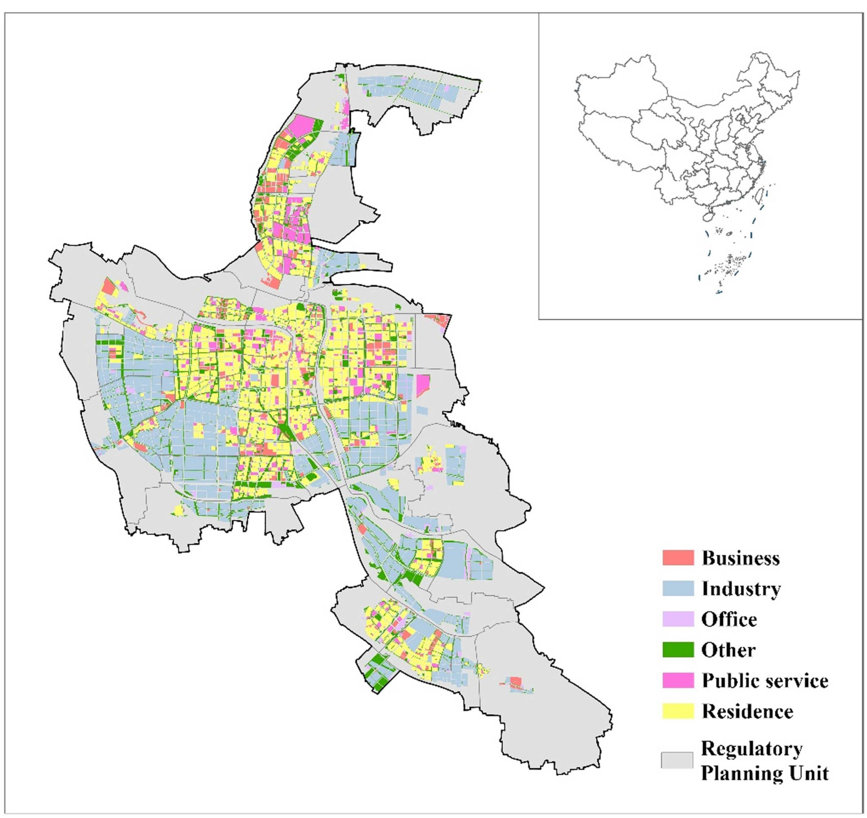

Figure 2. Study area.

Table 2. Data Souce.

Data type	Content summary	Source
Mobile Signalling Data	Full-day data on May 16, 2024; over 1.36 million records	China Mobile
POI Data	Acquired in Nov. 2024; 15 categories (e.g. dining, companies, shopping, finance); 140,000 + entries	Gaode Map
Housing Price data	Housing coordinates, building count, FAR, and types	Anjuke
Building Data	Acquired in Apr. 2025; including function types (simplified into Business, Industry, Office, Other, Public Service, Residence);	A Multi-Attribute Building Dataset of China(Zhang, Zhao, and Long 2025)
Land Use Data	Acquired in Nov. 2024; including land use types (simplified into Business, Industry, Office, Other, Public Service, Residence); 9,680 entries	Suqian Bureau of Natural Resources
Questionnaire Data	Conducted from March 13 to March 18, 2025, across various regulatory planning units in the central urban area of Suqian. A total of 1,028 questionnaires were distributed, with 952 valid responses collected. Over 90% of the respondents were aged between 18 and 50.	Field Survey

grained analysis of commuting behaviour and its spatial heterogeneity across the city. According to the survey, residents primarily commute by e-bike (45.8%) and private car (32.5%), the remaining commute modes include walking (8.1%), bicycle (3.8%), bus (6.7%), and ride-hailing (2.0%). Overall commuting durations are relatively long, with long-distance commutes mainly occurring along north-south corridors. The main commuting challenges include infrequent bus services, severe traffic congestion, and difficulties in finding parking for private cars. Figure 3 shows distribution frequencies of various commuting modes.

3.3 Data processing

Based on the conceptual framework of land use mix discussed in Section 2.2, the following indicators are constructed to quantify its spatial and functional characteristics from both two-dimensional and three-dimensional perspectives. Accordingly, this study develops independent variables across six dimensions: Diversity, Compatibility, Accessibility, Balance, Dynamic Commute, and Socioeconomic Feature, which together capture the comprehensive spatial, functional, and temporal attributes of mixed land use. All indicators were calculated at the level of Traffic Analysis Zones (TAZs), with a total of 147 zones covering the central urban area of Suqian. Each TAZ serves as the basic operational unit for quantifying the spatial and functional characteristics of land use mix. The computation of 2D and 3D indicators, including Diversity, Accessibility, and Compatibility, was implemented in Python 3.10 using the libraries GeoPandas, and NumPy, while spatial preprocessing and visualisation were conducted in ArcGIS Pro 3.2. The Dynamic Commute indicator was derived from commuting survey data through Python-based data processing and aggregation, and all variables were standardised within the same TAZ framework before modelling. The statistical summary of these variables is presented in Table 3.

3.3.1 Dependent variables

The dependent variable in this study is residents' commute mode choice. The majority of residents commute by e-bike (45.8%) and private car (32.5%), followed by walking (8.12%), bicycle (3.76%), public transit (6.67%), and ride-hailing (1.94%). Variance Inflation Factor (VIF) was used to test for multicollinearity. Since all VIF values were below 5, no multicollinearity was detected.

3.3.2 Independent variables

In this study, we compute a series of explanatory variables to quantify built environment characteristics and socioeconomic context, grouped into five categories: Diversity, Compatibility, Accessibility, Dynamic commutes, and Socioeconomic Features. Below we detail the definition and calculation of each variable in these categories.

3.3.2.1 Diversity. Diversity in land use mix refers to the proportional area of different land uses, such as residential, public service, and industrial areas (Hendrigan and Newman 2017). The typical Shannon index can only reflect balance, but it does not capture richness or aggregation (Krizek 2003). However, Hill Numbers can assess land use mix from a comprehensive perspective of richness, balance, and aggregation, including species richness, Shannon entropy, and Simpson concentration indicators (Yue et al. 2016; Yang,

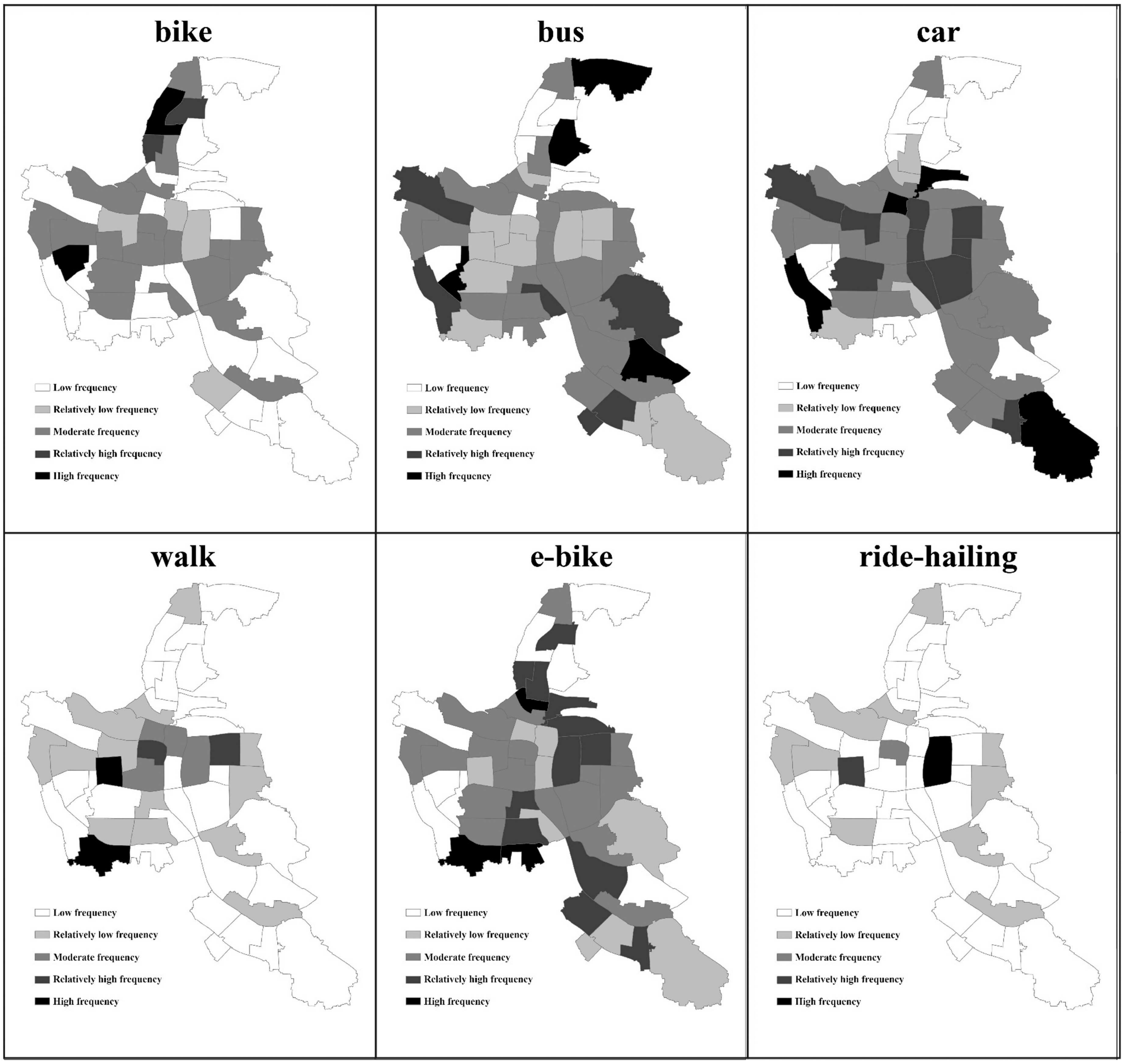

Figure 3. Commuter mode choice frequency profile.

Chung, and Kim 2021). Therefore, Hill Numbers perform better in measuring land use mix and this study uses the three-dimensional Hill index for measurement (Zhao, Xia, and Li 2023).

To comprehensively capture the degree of functional heterogeneity within each planning unit, this study adopts a 3D Diversity indicator based on the Hill Numbers framework. Unlike traditional two-dimensional indices, which rely solely on land parcel areas, the 3D approach incorporates both horizontal land area and vertical built-up intensity, thereby offering a more realistic representation of urban spatial complexity.

The generalised Hill Numbers (Wu et al. 2018) are expressed as:

$$^{q}DI_{2D} = \left(\sum_{k=1}^{\theta} P_k^q x \right)^{1/(1-q)} \tag{1}$$

where θ is the number of land use categories, and P_k is the proportion of land type k. When q = 0, the indicator measures richness (the number of land use categories); when q = 1, it approximates the exponential of the Shannon entropy, reflecting balance; when q = 2, it equals the inverse of the Simpson index, representing aggregation.

To extend this measure into three-dimensional space, we replace P_k with a floor-area-weighted land area ratio (M_k):

Table 3. Descriptive statistics for dependent and independent variables.

Categories	Variables	Mean	SD.	Min.	Max.
Dependent variables					
Commute Mode Choice	bike	0.057	0.069	0.008	0.435
	bus	0.053	0.058	0.000	0.312
	car	0.325	0.122	0.000	0.715
	walk	0.056	0.065	0.000	0.196
	e-bike	0.460	0.180	0.121	1.000
	ride-hailing	0.006	0.0104	0.000	0.044
Independent variables					
Diversity	3D Richness	1.879	1.425	0.000	6.000
	3D Balance	1.442	0.586	1.000	4.295
	3D Aggregation	1.330	0.481	1.000	3.893
Compatibility	2D Compatibility	0.502	0.239	0.000	1.000
	3D Compatibility	0.629	0.323	0.000	1.000
Accessibility	2D Accessibility	38.649	19.507	4.083	160.469
	3D Accessibility	343.083	480.718	1.660	2681.534
Balance	Job-Housing balance	0.347	0.179	0.001	0.981
	Retail-Housing balance	0.579	0.380	0.000	1.000
Dynamic commute	Average AM peak commute time (s)	3091.66	2026.99	0.00	16447.00
	Average AM peak commute distance (m)	20647.69	16873.32	0.00	111836.34
	Average PM peak commute time (s)	2998.33	1652.613	0.00	14010.00
	Average PM peak commute distance (m)	19558.98	16059.41	0.00	133156.26
Socioeconomic Feature	Average housing price (yuan)	6816.2	2903.5	1607.0	20550.0
	Proportion of young people (%)	0.185	0.106	0.000	0.783
	Proportion of females (%)	0.636	0.246	0.004	1.000
	Proportion of highly educated individuals (%)	0.335	0.259	0.000	0.999
	Proportion of car ownership (%)	0.795	0.209	0.069	1.000

$$M_k = \frac{A_k \times FA_k}{\sum_{k=1}^{\theta} (A_k \times FA_k)} \tag{2}$$

where A_k denotes the land parcel area of type k, and FA_k denotes its total floor area. This adjustment accounts for land parcels with limited ground coverage but substantial vertical development, such as high-rise residential and commercial complexes, whose functional impacts would otherwise be underestimated in 2D measures.

Accordingly, the 3D Hill Numbers are defined as:

$$^{q}DI_{3D} = \left(\sum_{k=1}^{\theta} M_k^{q} \right)^{1/(1-q)} \tag{3}$$

Specifically, $^{0}DI_{3D}$ captures the richness of land use types, $^{1}DI_{3D}$ reflects the balanc**e** of land use distribution, and $^{2}DI_{3D}$ indicates the aggregation degree of land use in 3D space. By integrating both horizontal and vertical information, the 3D Diversity indicator provides a more robust and accurate measure of the heterogeneity of urban land use mix compared with conventional 2D indices.

3.3.2.2 Accessibility. Accessibility measures the spatial proximity between different land uses. Typical methods for measuring accessibility include distance metrics, gravity-based models, and cumulative opportunity (Vale, Saraiva, and Pereira 2016). Distance metrics directly represent proximity through spatial distance (Abdullahi et al. 2015), without considering range limitations or distance decay effects. Gravity-based models assume that the spatial effect or attraction of different destinations decays with distance and time, but the choice of decay function significantly affects accessibility (Luo and Wang 2003). Cumulative opportunity identifies isochrones of travel costs, applies range limitations, and then calculates the number of opportunities within each isochrone (Palacios and El-Geneidy 2022). Cumulative opportunity is easier to calculate and interpret, making it suitable for measuring accessibility in land use mix. This study adopt the cumulative opportunity method with a "15-minute life circle" threshold (1.5 km radius, walking speed 1.67 m/s).

For 2D accessibility:

$$T_{ia}^{2D} = \frac{d_{ia}}{1.67},\ O_i^{2D} = \sum_{a} w_{ia}^{2D},\ AI^{2D} = \frac{1}{\mu} \sum_{i=1}^{\mu} O_i^{2D} \tag{4}$$

In Equation (4), $T_{ia}^{2D} = \frac{d_{ia}}{1.67}$ represents the two-dimensional distance between land-use unit i and functional type a, where d_{ia} denotes the horizontal distance and 1.67 is a decay coefficient used to standardise the distance scale. $w_{i\alpha}^{2D}$ indicates the weighted accessibility from unit i to function α, reflecting the effect of distance attenuation or service attraction. O_i^{2D} is the overall accessibility value of unit i, calculated as the sum of all weighted connections with different functional types. μ represents the total number of spatial units, and AI^{2D} denotes the mean 2D accessibility index across all units, describing the overall level of functional proximity within the study area.

For 3D accessibility, vertical travel time is added:

$$T_{i\beta}^{3D} = \frac{d_{i\beta}}{1.67} + \frac{h_{i\beta}}{1.5},\ O_i^{3D} = \sum_{\beta} w_{i\beta}^{3D},\ AI^{3D} = \frac{1}{\mu}\sum_{i=1}^{\mu} O_i^{3D} \tag{5}$$

In Equation (5), $T_{i\beta}^{3D} = \frac{d_{i\beta}}{1.67} + \frac{h_{i\beta}}{1.5}$ measures the three-dimensional distance between unit i and functional type β, combining both horizontal distance $d_{i\beta}$ and vertical distance $h_{i\beta}$. The coefficients 1.67 and 1.5 serve as decay factors for horizontal and vertical distances, respectively, to maintain dimensional consistency. $w_{i\beta}^{3D}$ represents the three-dimensional weighted accessibility, indicating the influence of different functional types on unit i in vertical and horizontal space. O_i^{3D} refers to the overall 3D accessibility value for unit i, and μ denotes the total number of units. Finally, AI^{3D} is the average three-dimensional accessibility index, reflecting the overall connectivity and interaction intensity among urban functions in 3D space.

3.3.2.3 Compatibility. Compatibility refers to the potential for different types of land uses to coexist in the same area, and it is an important indicator for measuring land use mix (Zhuo et al. 2019). High compatibility means that different land use types can coexist harmoniously, while low compatibility may lead to environmental pollution and social conflicts (Burnell 1985). Compatibility is primarily used to assess the degree of interaction between different land use types. The Mix Degree Index (MDI) represents the compatibility between residential and industrial land uses (Tian, Liang, and Zhang 2017), while the compatibility of all land use types can be expressed more accurately using the vector-based MDI (VMDI) and the weighted VMDI (WVMDI), which incorporates land area proportions (Zhuo et al. 2019). These indices provide a more precise representation of the compatibility of land use mix within an urban area. In summary, this study characterises 2D and 3D land use mix primarily from three dimensions: diversity, accessibility, and compatibility.

Compatibility indicators assess the spatial coexistence of diverse land-use types. Specifically, high compatibility signifies functional synergies such as those between residential and commercial areas, while low compatibility denotes intrinsic conflicts, typically exemplified by the proximity of residential zones to heavy industrial sites. A compatibility judgement matrix for different land use types was constructed, and land use was classified into six categories: Business, Industry, Office, Other, Public Service, and Residence. Table 4 presents the compatibility coefficients of the matrix, including coefficients for compatibility (0), conditional compatibility (0.5), and incompatibility (1).

For 2D Compatibility, using land area ratio P_j as the weight:

$$LCI_i^{2D} = 1 - \frac{\sum_j (C_{ij} \cdot P_j)}{\sum_j P_j},\ SCI^{2D} = \sum_{i=1}^{\mu} (P_i \cdot LCI_i^{2D}) \tag{6}$$

In Equation (6), LCI_i^{2D} represents the local compatibility index of land-use unit i. It measures the degree to which different land-use types within the unit can coexist harmoniously. C_{ij} denotes the compatibility coefficient between land-use type i and adjacent type j, which reflects the level of functional conflict or coordination between the two types. P_j refers to the land area ratio of type j, which is used as the weighting factor in the calculation. The numerator $\sum_j (C_{ij} \cdot P_j)$ represents the weighted average compatibility of

Table 4. Compatibility judgement matrix between different land use types.

	Business	Industry	Office	Other	Public service	Residence
Business	0	0.5	0	0.5	0	1
Industry	0.5	0	0.5	0.5	1	1
Office	0	0.5	0	0.5	0	1
Other	0.5	0.5	0.5	0	1	1
Public service	0	1	0	1	0	0.5
Residence	1	1	1	1	0.5	0

surrounding land uses, while the denominator $\sum_j P_j$ ensures normalisation across different area proportions. The value of LCI_i^{2D} decreases as land-use conflicts increase.

SCI^{2D} is the spatial compatibility index for the entire study area, calculated as the weighted sum of all local compatibility values. P_i is the land area ratio of unit i, and μ denotes the total number of land-use units. This indicator reflects the overall degree of spatial coordination and functional integration of land uses across the study area.

For 3D Compatibility, Replacing P_j with the floor-area-weighted land ratio M_j:

$$LCI_i^{3D} = 1 - \frac{\sum_j (C_{ij} \cdot M_j)}{\sum_j M_j}, \; SCI^{3D} = \sum_{i=1}^{\mu} (M_i \cdot LCI_i^{3D}) \tag{7}$$

With

$$M_j = \frac{A_j \cdot FA_j}{\sum_j (A_j \cdot FA_j)} \tag{8}$$

In Equation (7), LCI_i^{3D} represents the local 3D compatibility index of land-use unit i. It measures the degree of spatial and functional harmony among different land uses in three-dimensional space. C_{ij} denotes the compatibility coefficient between land-use type i and adjacent type j, reflecting the level of functional coordination or conflict between them. M_j represents the building volume of type j, which is calculated as the product of parcel area (A_j) and floor area (FA_j). This volumetric factor serves as a weight that captures the built-up intensity of each land-use type. The numerator $\sum_j (C_{ij} \cdot M_j)$ represents the weighted compatibility of surrounding land uses, while the denominator $\sum_j M_j$ normalises the measure across units with different building volumes. A smaller LCI_i^{3D} value indicates a higher degree of spatial conflict among vertical land uses.

SCI^{3D} denotes the spatial compatibility index of the entire study area, calculated as the weighted sum of all local 3D compatibility values. M_i represents the building volume of unit i, and μ refers to the total number of land-use units. By incorporating the volumetric factor, the 3D indicator captures the influence of built-up intensity and provides a more accurate representation of land-use compatibility in high-density urban environments.

3.3.2.4 Balance. Balance characteristics such as job–housing balance and retail–housing balance not only reflect the degree of land use mix but are also closely linked to travel behaviour. Job–housing balance is widely used to measure the spatial match between employment opportunities and residential populations, with higher levels generally associated with shorter commuting distances and improved travel efficiency. Retail–housing balance, in turn, captures the distribution of service facilities around residential areas and can reduce travel demand and alleviate traffic pressure (Zhang and Zhao 2017).

The Job-Housing Balance measures the balance between residential and employment areas within a city or region. It is calculated using mobile signal data, where the start and end grid locations represent residential and employment areas, respectively. Specifically, the number of departures from a grid during the morning peak (e.g. 6:00-9:00 AM) represents the residential population, while the number of arrivals at a grid during the same period represents the employment population. The JHB is calculated as the ratio of residential to employment population.

Retail-Housing Balance measures the accessibility of retail services within a 5 km radius of residential areas, reflecting the proximity between residential and retail land uses. It is calculated as the ratio of shopping trips occurring within this radius to the total shopping trips, weighted by the number of trips. RH was computed using smartphone signalling data to identify residential locations, retail POI data for shopping destinations, and TAZ data. A higher RH value indicates better land-use integration, suggesting increased convenience for residents and potentially reduced transportation demand.

3.3.2.5 Dynamic Commute. Traditional measures of land use mix largely rely on static indicators such as the job–housing ratio, land use diversity, and floor area ratio, while overlooking residents' actual travel characteristics at different times of the day. In contrast, morning and evening peak hours, as concentrated commuting windows, more directly capture the interaction between land use and commuting behaviour (Gehrke and Clifton 2016). Commute time and distance during these periods not only reflect the degree of functional matching but also serve as indicators of urban operational efficiency: well-integrated land use is typically associated with shorter commutes and lower traffic pressure, whereas spatial mismatch manifests as prolonged commuting and pronounced tidal flows. Moreover, peak-hour commuting features often exhibit nonlinear and threshold effects, such as moderate job–housing balance reducing commute distances, while excessive concentration may create bottlenecks. Dynamic indicators therefore provide stronger explanatory power than static land-based measures, revealing critical thresholds and offering planners practical insights for identifying areas where land use mix fails to alleviate peak-hour congestion.

The four indicators, Average AM peak commute time, Average AM peak commute distance, Average PM peak commute time, and Average PM peak commute distance, are selected as dynamic commutes because they capture temporal variations in commuting behaviour during peak hours. These periods, both morning and evening, are essential for understanding the changes in travel demand, which are influenced by factors such as land use, accessibility, and infrastructure. By considering both time and distance, these indicators offer a comprehensive view of commuting intensity and efficiency. Their inclusion provides insights into how commuter behaviour evolves throughout the day, highlighting the dynamic nature of urban mobility.

3.3.2.6 Socioeconomic Feature. To capture the influence of socioeconomic conditions on commute mode choice, five indicators were selected under the Socioeconomic Feature dimension: average housing price, proportion of highly educated residents, proportion of females, proportion of young people, and car ownership rate (Dong et al. 2023). These indicators were derived from housing data and questionnaire responses at the TAZ level. Average housing price reflects economic status and residential affordability; education level, gender, and age structure capture key demographic characteristics associated with travel preferences; and car ownership rate directly affects access to motorised transport modes.

4 Methodologies

4.1 XGBoost

XGBoost is an efficient machine learning algorithm based on the Gradient Boosting Decision Tree (GBDT) framework. It optimises the loss function using a second-order Taylor expansion, incorporating both first and second derivatives to improve model adaptation and accuracy. The objective is to minimise the following loss function:

$$L(\phi) = \sum_{i=1}^{n} l(y_i, \hat{y}_i) + \sum_{k=1}^{K} \Omega(f_k) \tag{9}$$

where $l(y_i, \hat{y}_i)$ is the loss function and $\Omega(f_k)$ is the regularisation term for model complexity. XGBoost builds an ensemble of decision trees, minimising errors for better predictions.

4.2 SHAP

In this study, we used the SHAP (SHapley Additive exPlanations) method to interpret the outputs of the XGBoost model. The SHAP method is based on Shapley value theory, which was originally used in game theory to measure the contribution of individual participants to the overall gain. In the field of machine learning, SHAP values are increasingly used to quantify the contribution of each feature to model predictions, thus clarifying the importance and impact of feature variables. The SHAP method calculates the contribution of each feature using the following formula:

$$\phi_i(f, x) = \sum_{S \subseteq N \setminus \{i\}} \frac{|S|!(|N| - |S| - 1)!}{|N|!} [f_x(S \cup \{i\}) - f_x(S)] \tag{10}$$

In the formula, ϕ_i represents the Shapley value for the feature x, f is the prediction function, x is the feature quantity, N is the set of all features, and S is a subset of features. This formula adds the marginal contribution of a feature when added to all possible combinations of the remaining features to ensure a fair distribution of the predicted contribution.

The advantage of SHAP explanations lies in its interpretability. SHAP values are based on the concept of Shapley values from game theory, which provides a unified framework for both local and global interpretations. In terms of local interpretation, SHAP values reveal how each feature influences the prediction of a single sample. For global interpretation, SHAP values across samples can be aggregated to understand the overall contribution of the model to different features.

5 Results and discussion

5.1 Relative importance of variables

Based on the regression model results, XGBoost was chosen as the preferred model because it outperformed others in most travel modes, especially for ride-hailing e-bike ($R^2 = 0.6999$, RMSE = 0.1158). While Random Forest (RF) performed best for car ($R^2 = 0.5537$), XGBoost showed more consistent performance across different modes and better captured complex nonlinear relationships. Linear Regression performed the worst, particularly for ride-hailing ($R^2 = 0.1397$) and bus ($R^2 = 0.1475$), indicating its inability to capture nonlinear effects. Although LightGBM performed similarly to XGBoost in some cases, it was slightly worse for ride-hailing ($R^2 = 0.3923$) and e-bike ($R^2 = 0.6931$). Therefore, XGBoost was chosen as the most suitable model for predicting travel mode choice.

To balance model complexity and predictive performance, we configured the XGBoost classifier with the following key hyperparameters: the number of boosting rounds (n_estimators) was set to 1200 to ensure sufficient learning capacity; the maximum tree depth (max_depth) was limited to 6 to prevent overfitting; and a moderate learning rate (learning_rate = 0.01) was chosen to ensure stable convergence. In addition, a fixed random seed (random_state = 42) was applied to guarantee reproducibility of results. This parameter setting provided a good trade-off between model accuracy and generalisation. Figure 4 presents the SHAP analysis of the impact of land use-related characteristics on different commuting modes.

In this study, socioeconomic characteristics played a crucial role in the selection of commuting behaviours. The proportion of highly educated individuals significantly influenced the choice of low-carbon travel modes, such as walking and e-biking. Highly educated groups tend to prefer environmentally friendly modes of transportation, reflecting their concern for health, the environment, and quality of life. Furthermore, the proportion of females positively affected the choice of public transport and e-bikes, potentially due to women’s higher demand for safety and convenience while travelling. In contrast to the younger and highly educated groups, middle-aged individuals relied more on private cars, reflecting their preference for time efficiency and comfort. The differences in socioeconomic characteristics highlight that commuting behaviour is influenced not only by urban accessibility and land use but also by individuals’ socioeconomic backgrounds.

From the perspective of 3D diversity, 3D Balance exhibits the strongest explanatory power. For commuting modes such as bus, car, and walking, its relatively high SHAP values suggest that when commercial, residential, and office functions are more evenly integrated within vertical spaces, residents are more inclined to adopt low-carbon travel modes rather than relying solely on private cars. This finding highlights the importance of functional equilibrium in three-dimensional land use, which directly contributes to reducing job–housing mismatch and promoting sustainable commuting. By contrast, 3D Richness and 3D Aggregation demonstrate considerably weaker explanatory power, with SHAP values clustered around zero. This indicates that neither the mere clustering of building forms nor the structural complexity of urban functions significantly alters commuting choices. Such results imply that urban planning strategies should prioritise vertical functional balance rather than focusing only on morphological richness or spatial concentration, which appear insufficient to influence commute mode choice in practice.

From the perspective of 3D diversity, both 2D and 3D Accessibility significantly affect commute mode choice, yet with distinct roles. 2D Accessibility exerts moderate explanatory power, primarily promoting the use of mechanised travel modes such as car, ride-hailing, and bus, while its effect on walking and e-bike travel remains weak. In contrast, 3D Accessibility demonstrates stronger explanatory power and clear nonlinear trends: higher 3D accessibility increases the likelihood of walking and cycling, while reducing reliance on private cars. These findings suggest that traditional planar measures of accessibility may underestimate the role of vertical urban structures, highlighting the necessity of incorporating 3D accessibility in planning strategies to foster low-carbon commuting.

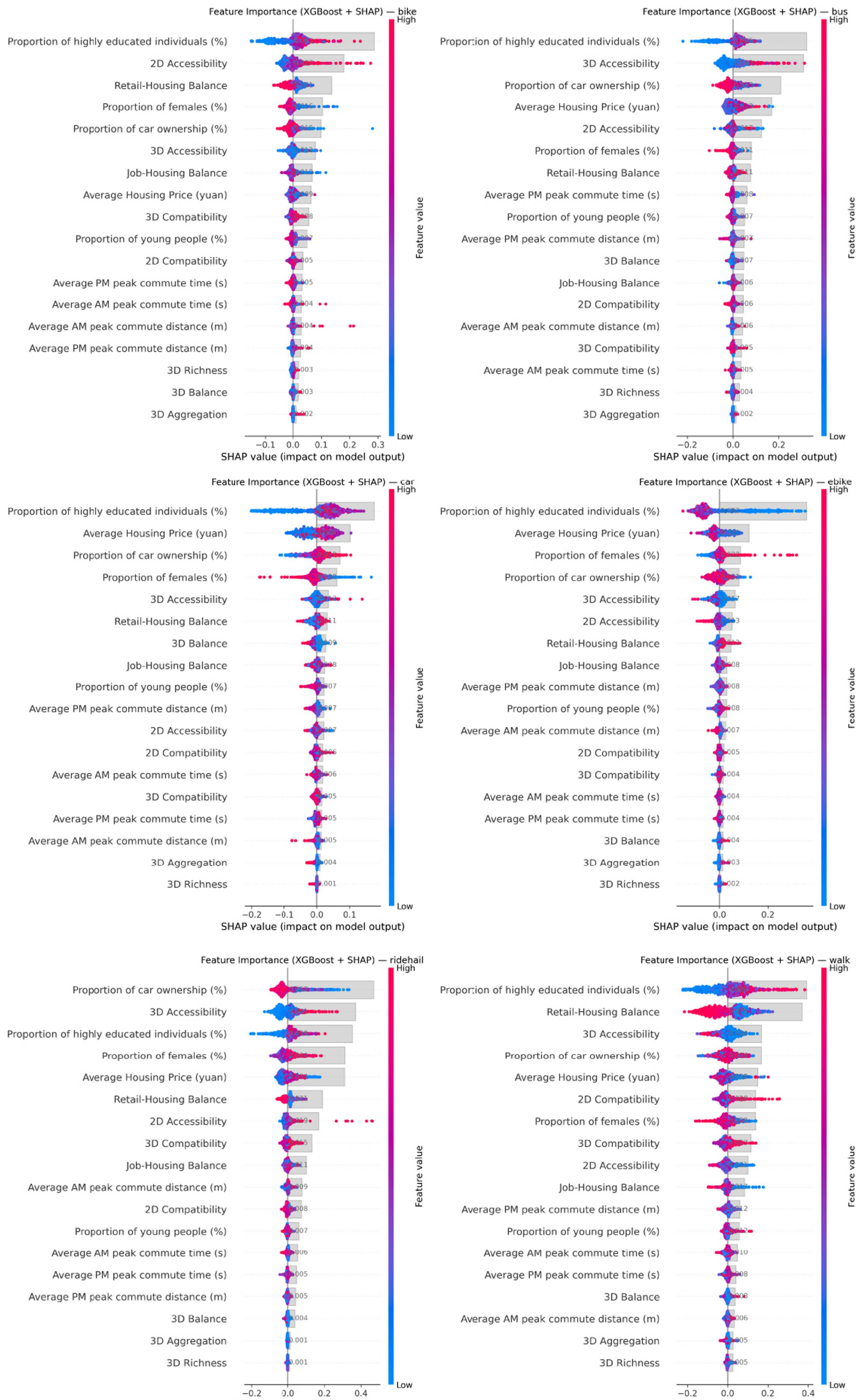

Figure 4. Combination of bee swarm and importance of independent variables; Bottom X-axis (Beeswarm Plot): Displays the distribution of SHAP values for each feature, with colours representing the magnitude of feature values. X-axis (Bar Chart): Each feature's average SHAP value serves as an importance ranking.

According to the SHAP results, both 2D and 3D Compatibility exhibit relatively low global importance compared with other indicators. For 2D Compatibility, SHAP values are tightly clustered around zero, with only minor deviations for bus and car modes, indicating weak explanatory power. In contrast, 3D Compatibility shows slightly higher importance and more dispersed SHAP values, particularly for bus and walking, suggesting that vertical functional compatibility exerts a more noticeable influence on low-carbon commuting modes. Nevertheless, the overall explanatory power of compatibility indicators remains limited across all travel modes.

From the perspective of dynamic commute, peak-hour commuting characteristics have moderate explanatory power, mainly for mechanised travel modes. Among the four indicators, commuting time during the PM peak exhibits the strongest influence, particularly for bus and car, as its SHAP values are more dispersed from zero. AM peak time also contributes, though to a lesser degree. In contrast, both AM and PM peak commuting distances display relatively weak explanatory power, with minor effects observed only for car. Overall, peak-hour commuting time is more informative than distance in explaining commute mode choice, while their influence on walking and non-motorised modes remains limited.

According to the SHAP results, Job–Housing Balance shows relatively high global importance and a wide distribution of SHAP values across multiple commuting modes, particularly car, bus, and e-bike. This indicates that its influence on commute mode choice is substantial and heterogeneous, with both positive and negative effects depending on local conditions. In contrast, retail–housing Balance exhibits relatively low global importance, with SHAP values clustered around zero and limited variation across modes, suggesting that its direct impact on commuting behaviour is weak. Overall, the comparison highlights that job–housing balance plays a more critical role in shaping commute mode choice, whereas retail–housing balance may primarily affect daily life convenience rather than commuting decisions.

5.2 The nonlinear relationship between land use mix variables and residents' commute mode choice

5.2.1 The nonlinear relationship between diversity and residents' commute mode choice

Among the 3D diversity indicators, 3D Richness and 3D Aggregation show SHAP values clustered around zero across all commuting modes, indicating that their explanatory power for commute mode choice is very limited. This suggests that the mere variety or spatial clustering of land-use types does not substantially affect residents' travel behaviour in the study area. Therefore, these two indicators are not discussed in detail here. In contrast, 3D Balance demonstrates markedly higher SHAP values and clear nonlinear effects across different modes, reflecting its critical role in capturing the functional equilibrium of land uses in vertical space. Hence, the following analysis focuses on the influence of 3D Balance, which represents the most meaningful dimension of 3D diversity in explaining commuting behaviour.

Figure 5 illustrates the nonlinear relationships between 3D Balance and commute mode choices. The SHAP dependence analysis shows that the effects of 3D Balance vary significantly across commuting modes, with particularly strong impacts on walking and car commuting. For walking, SHAP values are negative when 3D Balance is below 0.2 but turn positive once it exceeds 0.3; as the value increases further, the likelihood of walking rises, indicating that higher vertical functional balance facilitates walking. Cycling and e-bike use also show a slight upward trend with higher values, whereas car and bus commuting gradually decline. Overall, these results suggest that low levels of 3D balance tend to support automobile use, whereas higher levels increasingly promote sustainable travel modes such as walking and cycling. This conclusion is also consistent with the view of Kent et al., who argued that mixed land use combined with compact urban form is more conducive to sustainable travel behaviour (Kent et al. 2023).

5.2.2 The nonlinear relationship between accessibility and residents' commute mode choice

Figure 6 illustrates the nonlinear relationships between 2D Accessibility and commute mode choices. The partial dependence plot of 2D accessibility shows that the commuting rates of bike, ride-hailing, car, and bus travel increase with the improvement of 2D accessibility. However, the travel rates of walk and e-bike travel decrease as 2D accessibility improves. This indicates that with the enhancement of 2D accessibility, service facilities and transportation hubs become more concentrated, prompting people to choose more convenient transportation modes for commuting.

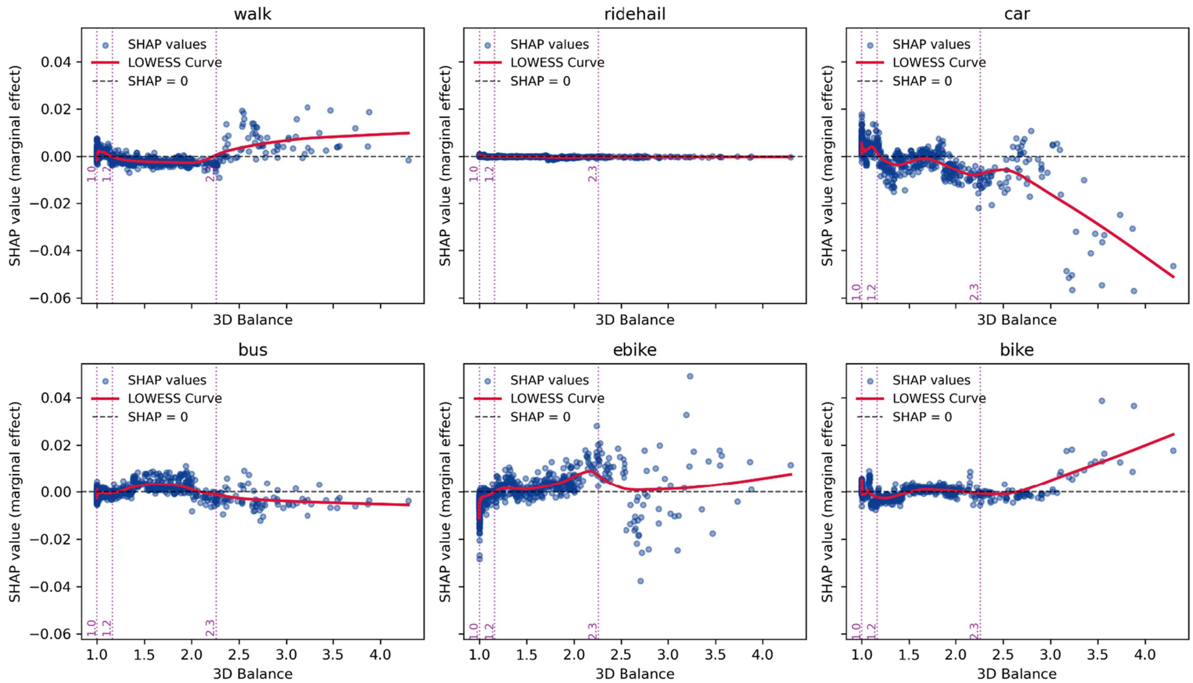

Figure 5. Nonlinear relationships between 3D Balance and commute mode choices.

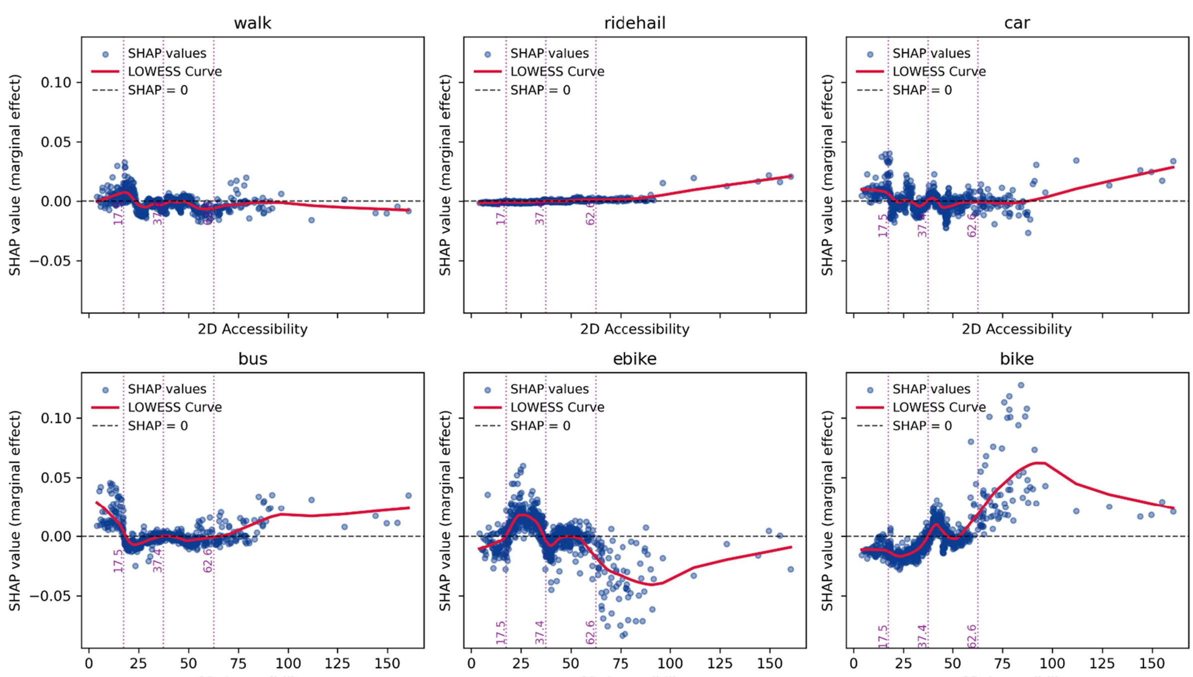

Figure 6. Nonlinear relationships between 2D Accessibility and commute mode choices.

Figure 7 illustrates the nonlinear relationships between 3D Accessibility and commute mode choices. From the partial dependence curve, 3D accessibility significantly impacts the choice of bus commuting, especially when vertical accessibility improves, leading to a significant increase in bus usage. Similarly, the proportion of walking and cycling also rises. Notably, the choice of ride-hailing services increases in areas with high 3D accessibility, reflecting a greater reliance on ride-hailing tools in high-density, high-rise

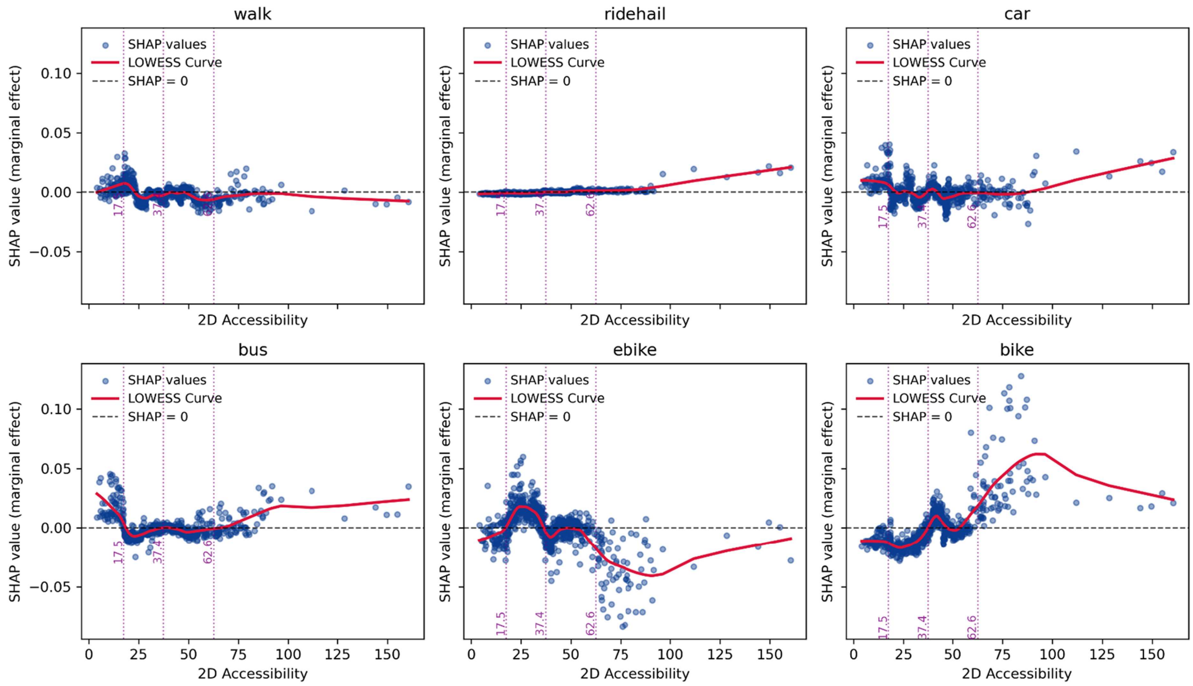

Figure 7. Nonlinear relationships between 3D Accessibility and commute mode choices.

environments. In this context, the commuting choice for e-mobility vehicles (such as e-bikes) declines. This may be due to higher traffic density and crowded spaces in these areas, which reduce the efficiency of using e-bikes. Additionally, tall buildings and busy streets may make cycling inconvenient, causing e-bike use to become less prioritised. People are more likely to choose ride-hailing tools like buses or ride-hailing to avoid traffic congestion and parking issues. This also indicates that in more refined and integrated measures of accessibility, including multimodal and temporal dimensions, improvements in accessibility are often accompanied by an increase in the share of public transit and ride-hailing modes (Chia and Lee 2020).

5.2.3 The nonlinear relationship between compatibility and residents' commute mode choice

Figure 8 illustrates the nonlinear relationships between 2D Compatibility and commute mode choices. The partial dependence analysis of 2D compatibility reveals that higher functional adjacency between parcels is associated with increased probabilities of walking commuting. E-bike usage remains the highest across all levels, indicating its flexibility under various compatibility scenarios. Notably, walking experiences a noticeable rise beyond a compatibility threshold of 0.5, implying that well-integrated horizontal land uses promote short-distance, non-motorised travel. Other modes such as car and bus remain relatively stable, showing less sensitivity to 2D compatibility variations.

Figure 9 illustrates the nonlinear relationships between 3D Compatibility and commute mode choices. The impact of 3D compatibility is more complex. As private car use declines, walking increases significantly, particularly in highly concentrated urban spaces where it becomes the dominant commuting mode. Meanwhile, ride-hailing shows an increase in areas with high 3D compatibility, reflecting the importance of ride-hailing in dense environments. Bicycle use also rises slightly in these areas, suggesting that vertically mixed spaces help promote low-carbon and green commuting behaviours such as walking and cycling.

5.2.4 The nonlinear relationship between dynamic commute and residents' commute mode choice

Figure 10 illustrates the nonlinear relationships between AM peak commute time (s) and commute mode choices. The SHAP dependence plots reveal that AM peak commute time exerts heterogeneous effects on travel modes. Walking is promoted under short commutes but strongly suppressed once the duration exceeds 50 minutes. Car use follows a similar pattern, showing slight promotion at short commutes but suppression at medium levels. As commute duration increases, the share of car trips first rises slowly and

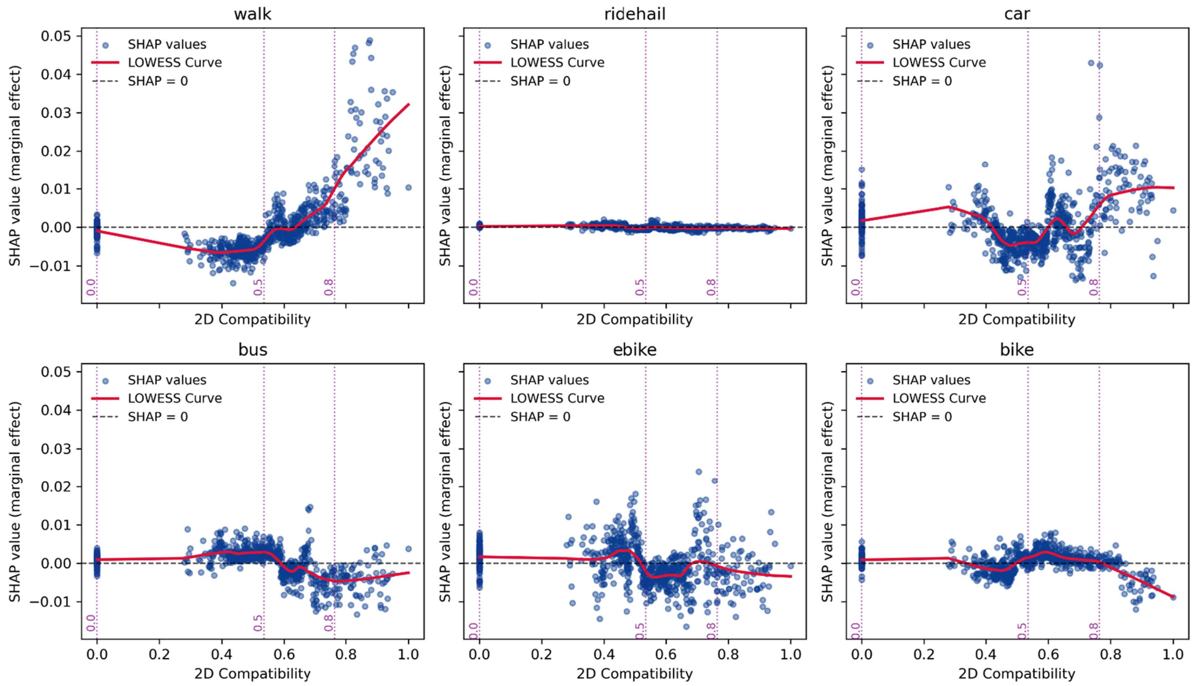

Figure 8. Nonlinear relationships between 2D Compatibility and commute mode choices.

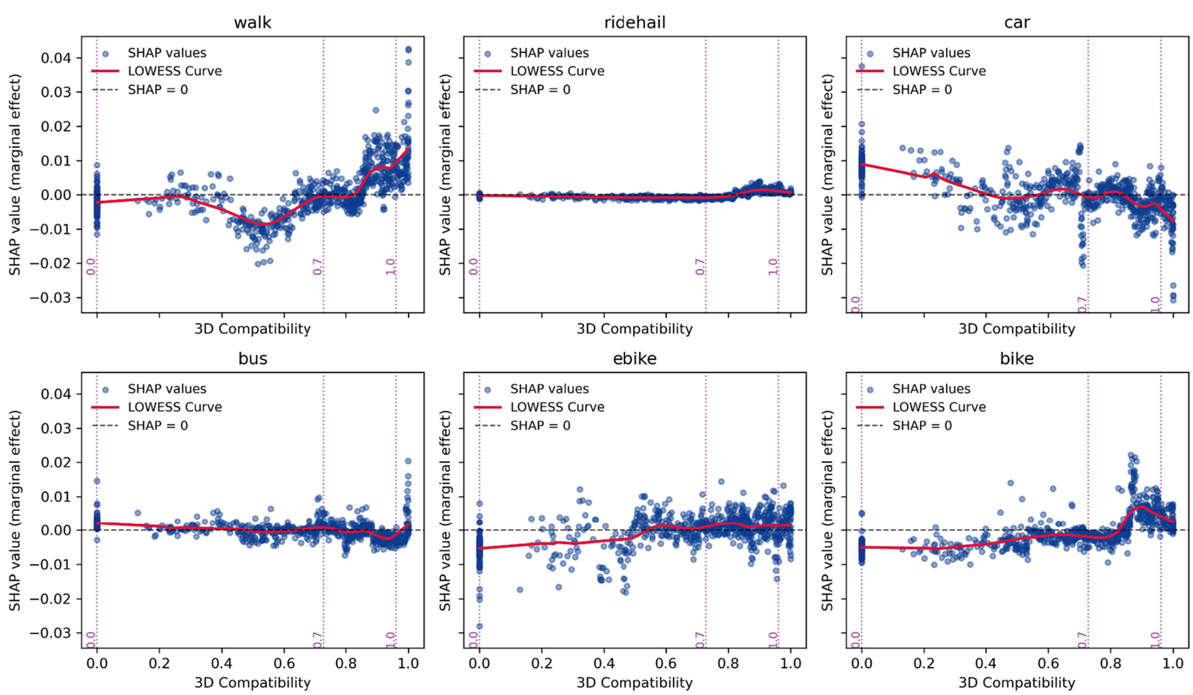

Figure 9. Nonlinear relationships between 3D Compatibility and commute mode choices.

then declines, but begins to increase again once the duration exceeds one hour. Public transit remains relatively stable across the entire range, showing a gradual upward trend. Bike appears neutral under short commutes, is suppressed at medium levels, and converges toward zero at longer durations. E-bike use shows almost no response. Overall, short commutes favour walking, cycling, and e-bike use, whereas longer commutes tend to encourage car and bus travel.

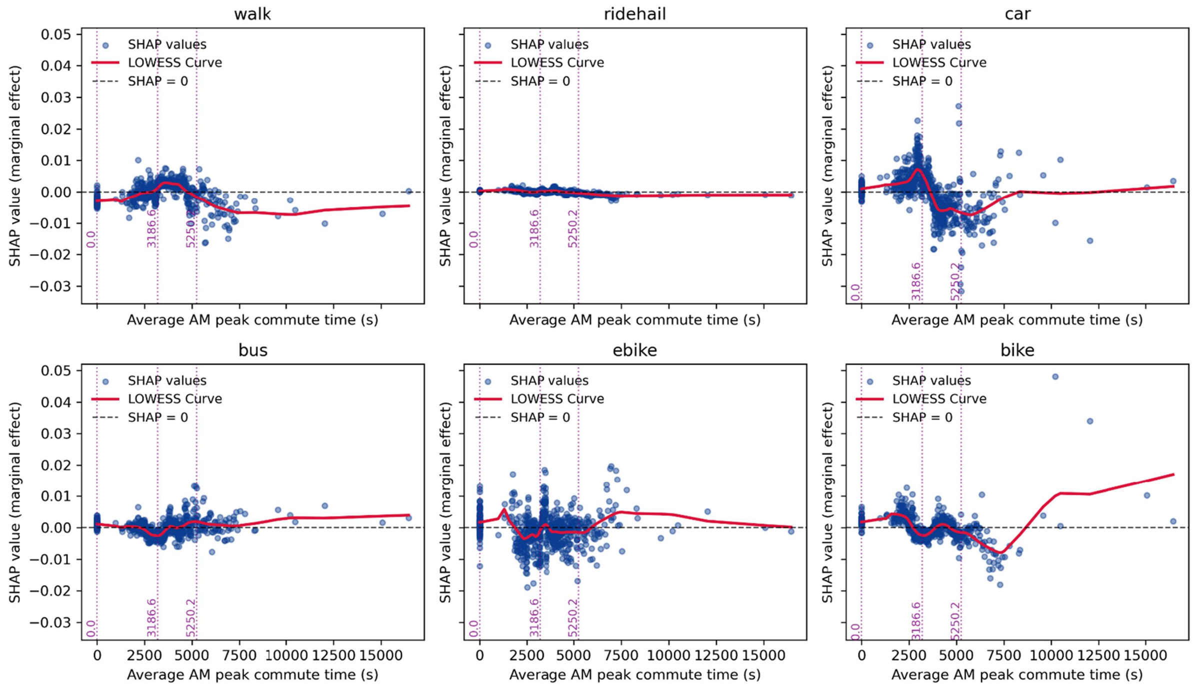

Figure 10. Nonlinear relationships between AM peak commute time (s) and commute mode choices.

Figure 11 illustrates the nonlinear relationships between AM peak commute distance (m) and commute mode choices. The SHAP dependence plots indicate that AM peak commute distance remains relatively stable overall. Walking and ride-hailing are virtually unaffected. Car use declines once commute distance exceeds 4 km, whereas bus travel shows a slight positive effect at longer distances beyond 4 km. E-bike use decreases after 2 km, reflecting its limitation to short-distance commuting. Cycling shows a mild negative effect at short to medium distances but turns positive at extreme distances greater than 6 km, which may be attributable to data sparsity. Overall, longer commute distances reduce car and e-bike use while slightly promoting bus travel, with negligible effects on walking and ride-hailing. In field investigations, it was found that the presumed reason is that many residents in Suqian work in townships or at local specialty enterprises (such as the Yanghe Distillery), which requires long-distance commuting by bus.

Figure 12 illustrates the nonlinear relationships between PM peak commute time (s) and commute mode choices. The dependency graph reveals that due to the limited data on long-duration commutes, the data fitting is problematic. Therefore, more accurate observations can only be made from commute data within 100 minutes. The choice rates for walking and cycling initially increase and then decrease as commute time rises, indicating that a commute duration of around 20 minutes best promotes walking and cycling. Electric bicycles have the highest usage rate, but their share declines consistently between 30 to 60 minutes, highlighting their limitations for medium-to-long commutes. The choice of car commuting shows a continuous upward trend within the 75-minute range, suggesting that longer commutes tend to encourage private car use. Bus commuting, on the other hand, is concentrated between 30 to 60 minutes. From this, it can be concluded that within a certain time range, an increase in commute duration tends to raise the probability of motorised transportation usage.

Figure 13 illustrates the nonlinear relationships between PM peak commute distance (m) and commute mode choices. The dependency graph reveals that due to the limited data on long-duration commutes, the data fitting is problematic. Therefore, more accurate observations can only be made from commute data within 100 minutes. The choice rates for walking and cycling initially increase and then decrease as commute time rises, indicating that a commute duration of around 20 minutes best promotes walking and cycling. Electric bicycles have the highest usage rate, but their share declines consistently between 30 to 60 minutes, highlighting their limitations for medium-to-long commutes. The choice of car commuting shows a continuous upward trend within the 75-minute range, suggesting that longer commutes tend to encourage private car use. Bus commuting, on the other hand, is concentrated between 30 to 60 minutes.

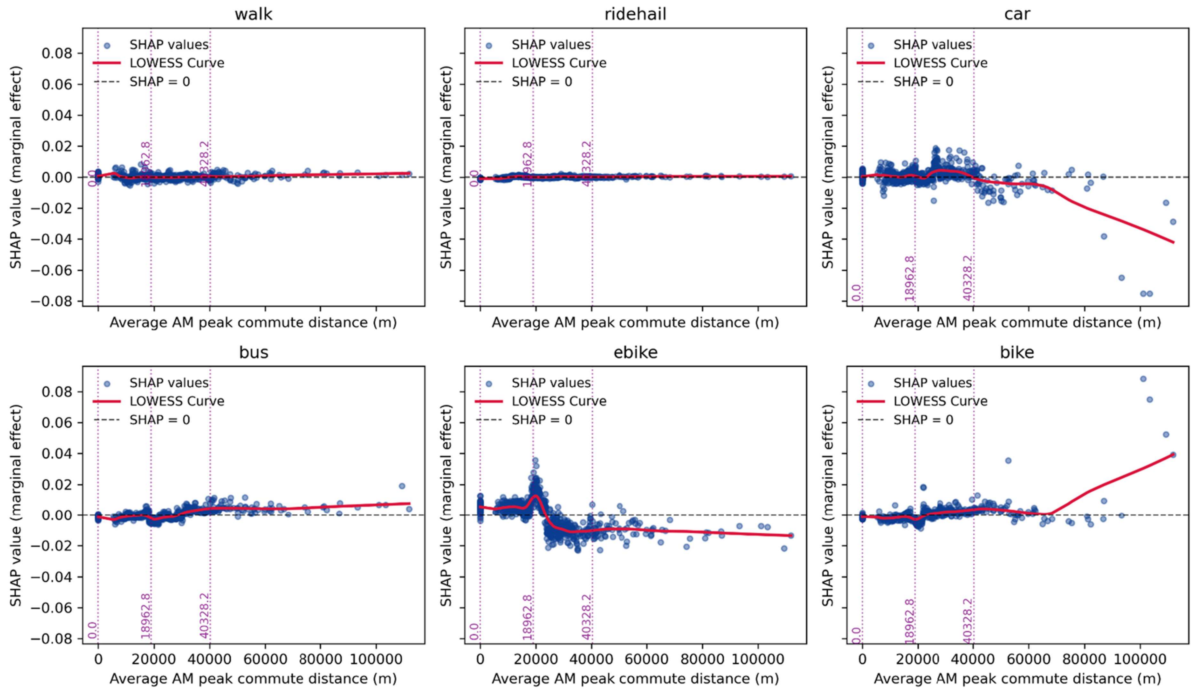

Figure 11. Nonlinear relationships between AM peak commute distance (m) and commute mode choices.

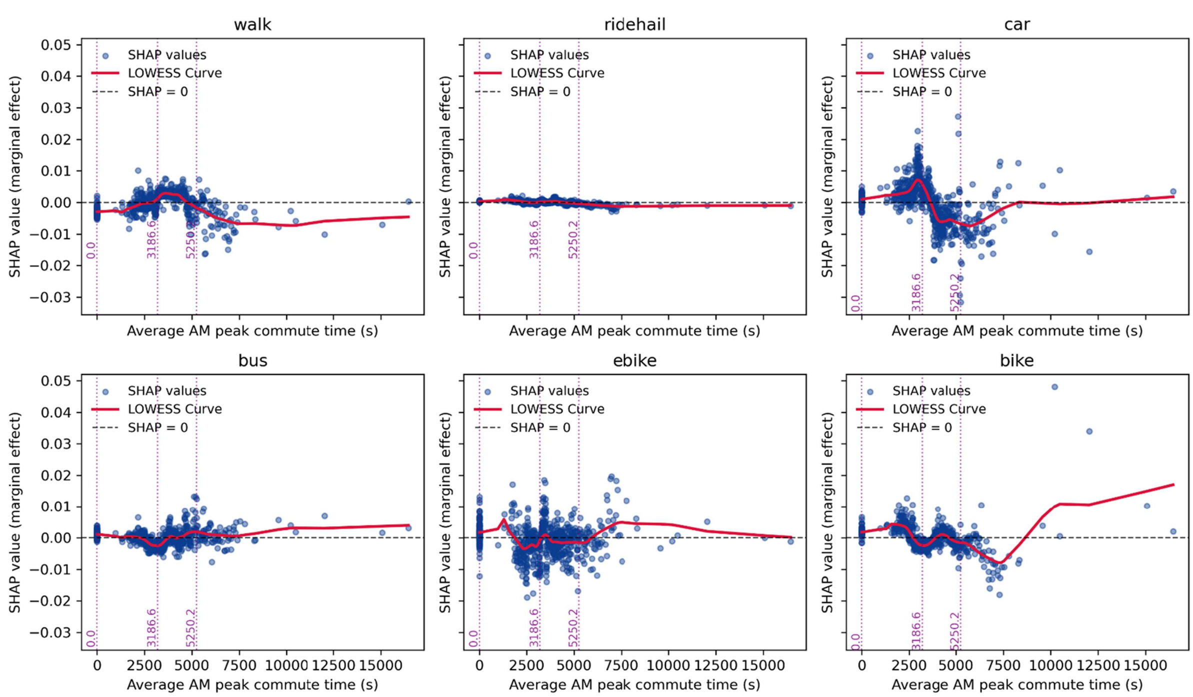

Figure 12. Nonlinear relationships between PM peak commute time (s) and commute mode choices.

From this, it can be concluded that within a certain time range, an increase in commute duration tends to raise the probability of motorised transportation usage.

5.2.5 The nonlinear relationship between balance and residents' commute mode choice

Figure 14 illustrates the nonlinear relationships between Job-Housing Balance and commute mode choices. From the partial dependence plot of job–housing balance, it can be observed that private car use is highest

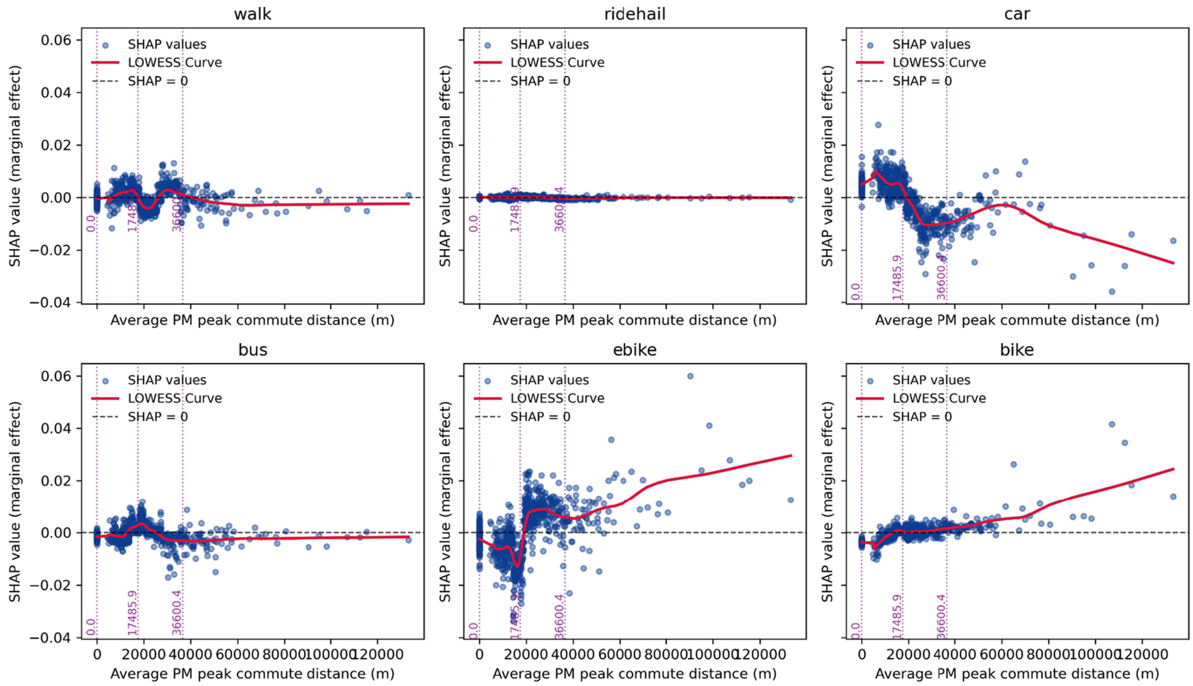

Figure 13. Nonlinear relationships between PM peak commute distance (m) and commute mode choices.

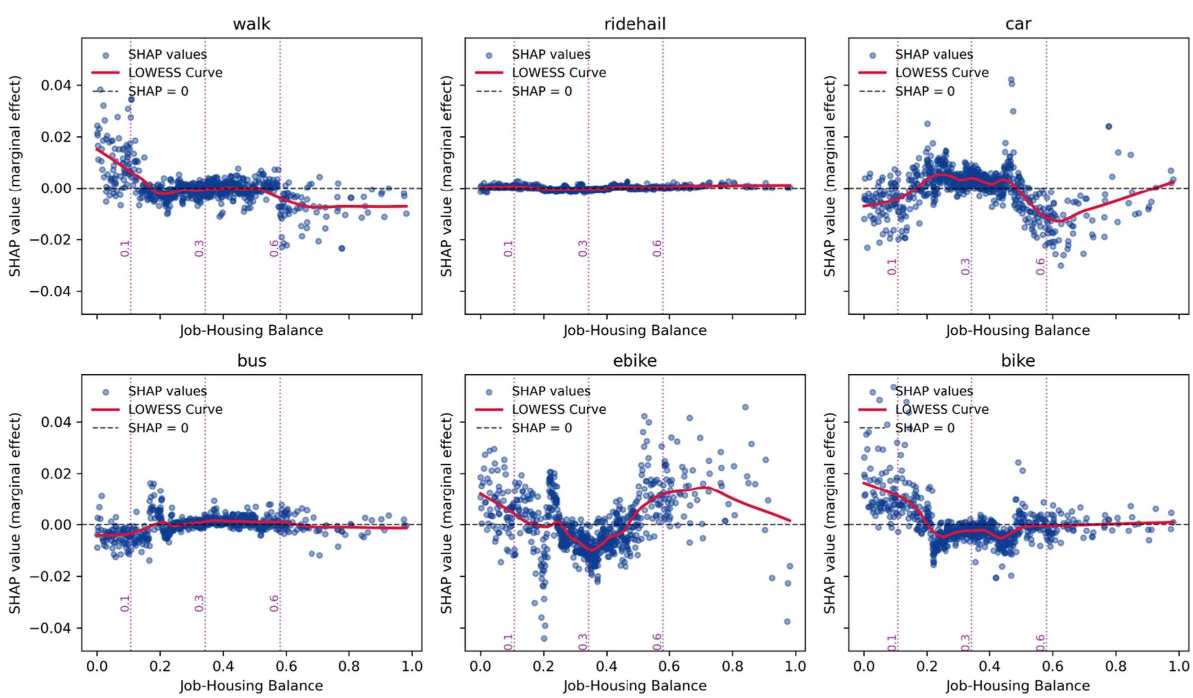

Figure 14. Nonlinear relationships between Job-Housing Balance and commute mode choices.

when the balance is low and gradually decreases as the balance improves. This indicates that when jobs and residences are spatially separated, people rely more on private cars to bridge the distance. Notably, e-bike use first decreases and then increases with rising job–housing balance, showing a clear turning point at around 0.4, where improved balance unexpectedly suppresses e-bike adoption. Beyond 0.5, the marginal effect becomes positive and peaks near 0.65, suggesting that e-bikes become more attractive under

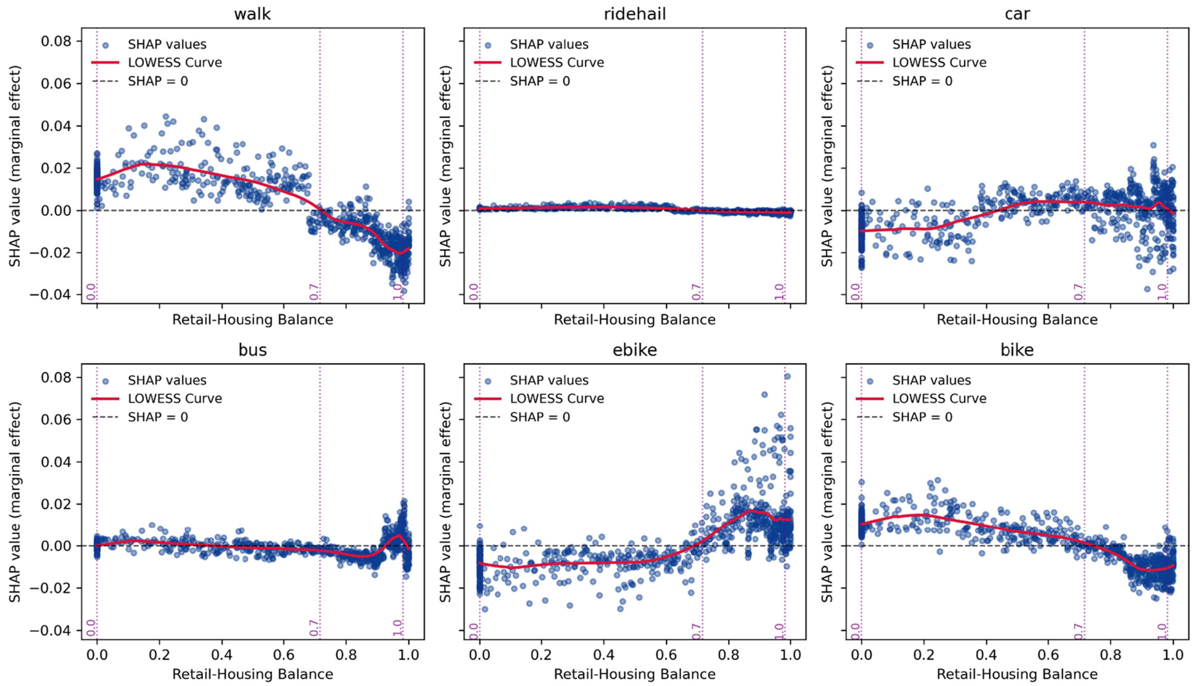

Figure 15. Nonlinear relationships between Retail-Housing Balance and commute mode choices.

medium-to-high levels of balance. This implies that as jobs and residences are more closely integrated, individuals are more likely to opt for low-carbon modes such as walking and cycling. Ride-hailing use remains relatively low with fluctuations across the balance range, indicating that it is less dependent on job–housing balance compared to other modes.

Figure 15 illustrates the nonlinear relationships between Retail-Housing Balance and commute mode choices. From the partial dependence plot of retail–housing balance, it is evident that the marginal effects vary substantially across commuting modes. Walking shows positive effects at low balance levels (0–0.2), but its marginal effect decreases steadily with higher balance and becomes strongly negative beyond 0.8, suggesting that highly coupled retail–housing environments may discourage walking. Bicycles also display positive effects under low balance but gradually shift into negative territory as the balance increases, following a similar trend to walking. In contrast, private car use exhibits stronger positive effects at higher balance levels, particularly above 0.8, indicating greater attractiveness in environments where retail and residential areas are closely integrated. E-bikes present positive effects under medium-to-high balance (0.3–0.7) and maintain positive contributions at higher levels, highlighting their adaptability to such spatial configurations. By comparison, bus and ride-hailing curves remain close to zero, suggesting that their use is not strongly dependent on retail–housing balance. Overall, lower levels of balance are more favourable for walking, whereas higher levels tend to promote e-bike commuting.

5.2.6 The nonlinear relationship between socioeconomic feature and residents' commute mode choice

Figures 16 to 20 illustrate the nonlinear relationships between five socioeconomic indicators and residents' commute mode choices. These five indicators are average housing price, proportion of young people, proportion of highly educated individuals, proportion of females, and proportion of car ownership. These variables generally exhibit higher SHAP values compared with spatial indicators, indicating that socio-economic attributes exert strong influences on commuting behaviour. For instance, higher housing prices are associated with increased walking and reduced private car use, while higher car ownership rates significantly promote private car commuting and suppress bus and e-bike use. Nevertheless, as this study primarily focuses on the spatial dimension of the built environment, socioeconomic factors are treated as supplementary control variables rather than the core subject of analysis. Therefore, while their overall importance is recognised, detailed interpretations of Figures 16 to 20 are omitted here, and the discussion remains centred on how 2D and 3D land use mix characteristics affect commute mode choice.

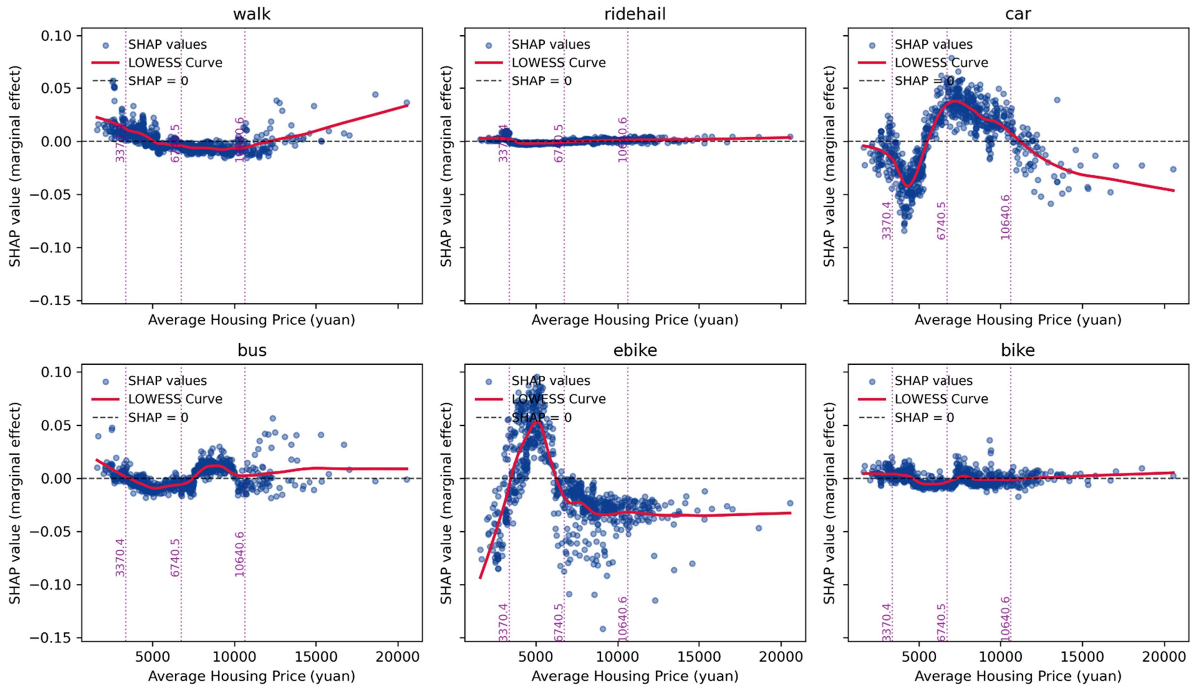

Figure 16. Nonlinear relationships between Average Housing Price (yuan) and commute mode choices.

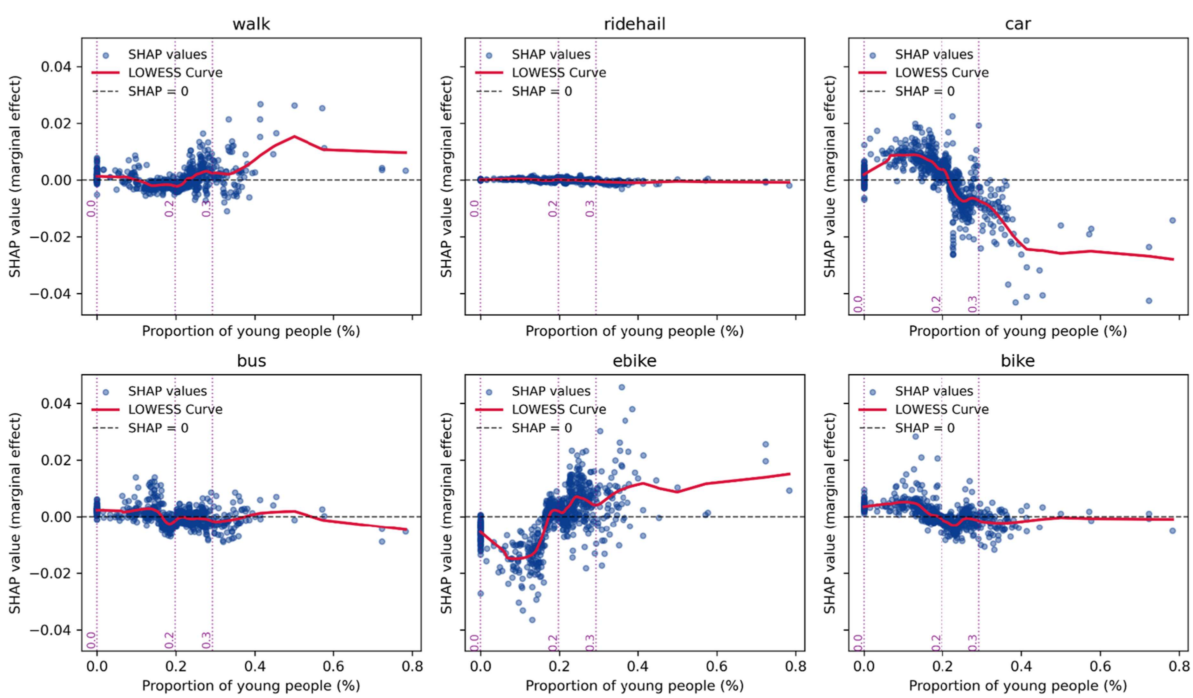

Figure 17. Nonlinear relationships between Proportion of young people (%) and commute mode choices.

6 Conclusion

Overall, this study advances research on the relationship between land use mix and commuting by extending the analytical framework from a traditional 2D perspective to an integrated 2D–3D approach. The results both confirm and expand prior findings: consistent with studies highlighting compactness and

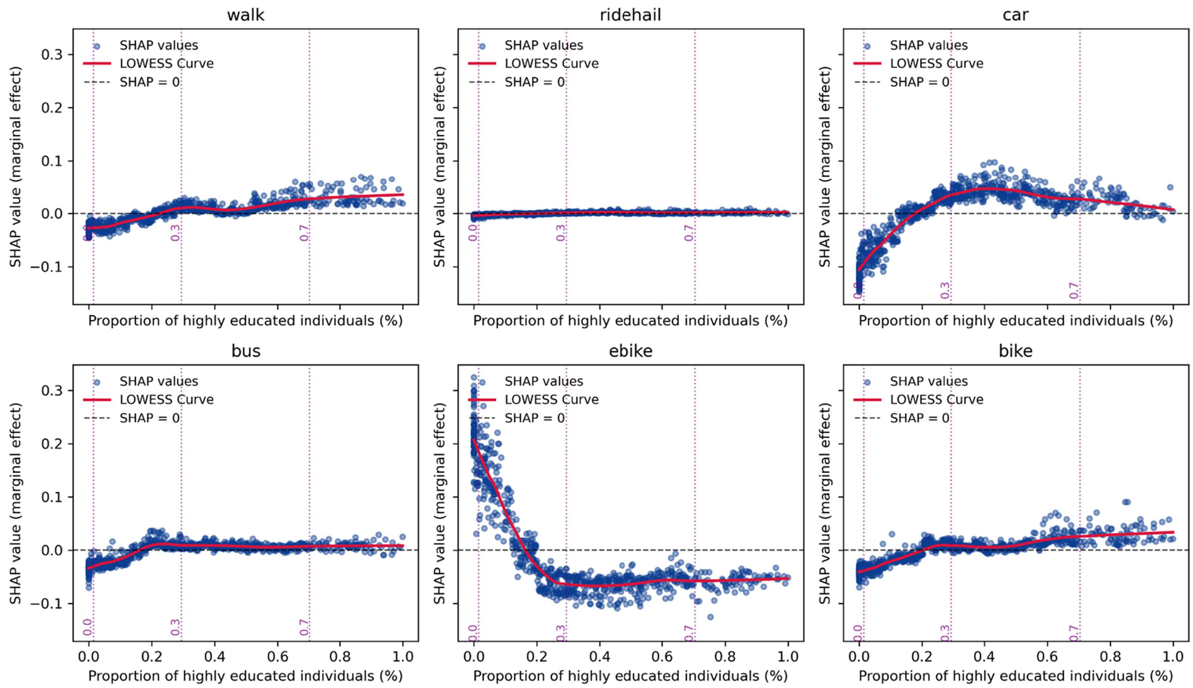

Figure 18. Nonlinear relationships between Proportion of highly educated individuals (%) and commute mode choices.

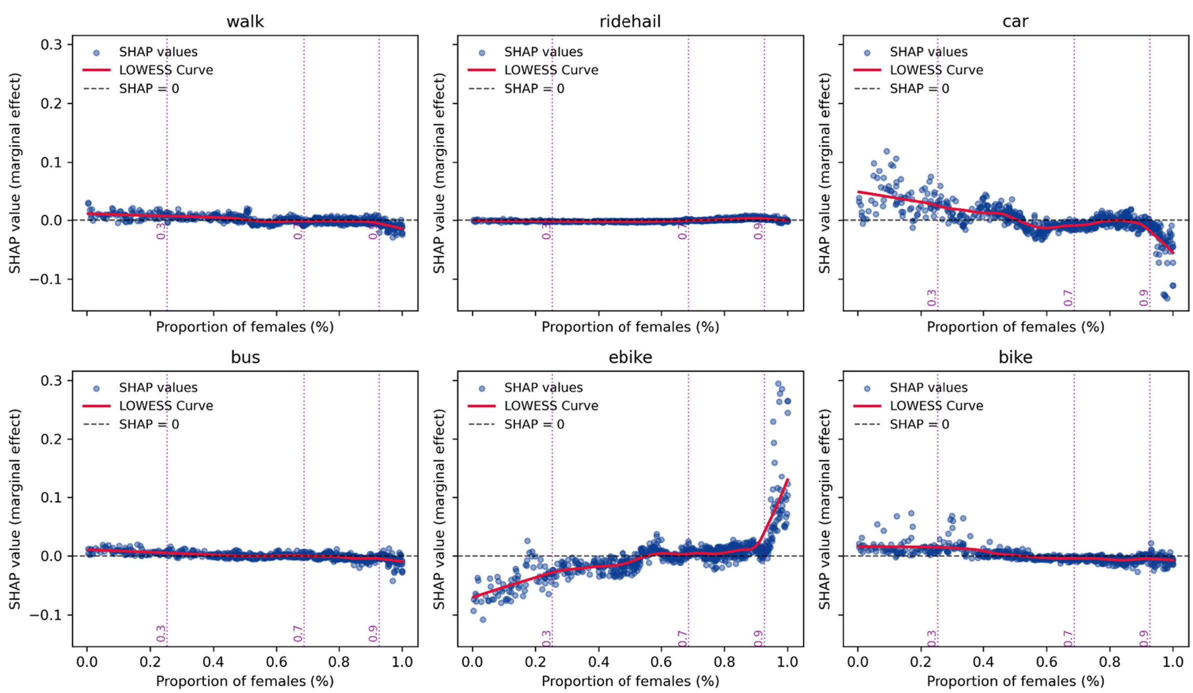

Figure 19. Nonlinear relationships between Proportion of females (%) and commute mode choices.

functional mix as drivers of sustainable mobility, the addition of 3D dimensions provides a more nuanced explanation of commuting differences in vertical urban space. Specifically, walking is suppressed when 3D Balance falls below approximately 0.2 but increases markedly once it exceeds 0.3, while private car use declines significantly when 3D Aggregation surpasses about 0.02. Both 2D and 3D Accessibility exert significant effects, yet 3D Accessibility shows stronger and nonlinear impacts in promoting walking and

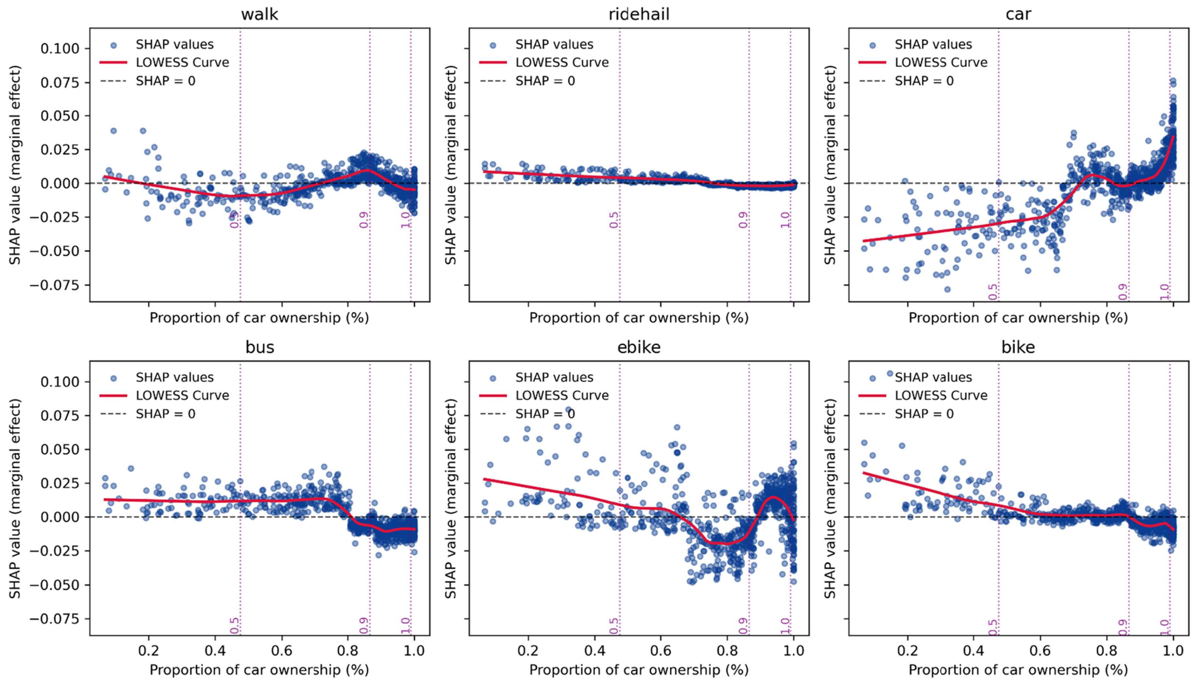

Figure 20. Nonlinear relationships between Proportion of car ownership (%) and commute mode choices.

cycling. These findings enrich earlier research by demonstrating that 3D indicators based on building volume and floor information, particularly 3D Balance and 3D Accessibility, better capture the influence of vertical stacking and functional equilibrium on commuting modes, avoiding the underestimation of high-rise complexes and overestimation of low-density land uses (Labetski et al. 2023; Xia et al. 2025). Incorporating dynamic commuting features further reveals that evening peaks impose the strongest constraints on mode choice, echoing prior discussions of "transport realities" while refining them through the identification of nonlinear thresholds. Theoretically, this study establishes a 2D–3D nonlinear analytical framework that advances built environment–mobility research paradigms; practically, it provides policy implications such as enhancing vertical job–housing integration (e.g. maintaining 3D Balance ≥ 0.3), promoting micro-renewal to reduce vertical impedance, and strengthening peak-hour public transit to mitigate congestion and foster low-carbon commuting.

Based on these findings, we propose the following policy recommendations:

(1) Vertical Functional Integration and Use Balance: In key areas, guide 3D Balance to ≥ 0.3, encouraging the vertical integration of residential, office, and commercial functions at the building or block scale, while prioritising the renewal of single-function clusters characterised by low balance and high land coverage.
(2) Enhancement of 3D Accessibility for Walking and Cycling; Job–Housing Coupling through Quotas and Assessment: Implement micro-renewal measures around public service and employment nodes (e.g. sky corridors, elevated pedestrian systems, slow-traffic bridges, three-dimensional signage, elevators/ramps) to reduce vertical impedance and enhance 3D Accessibility. At the same time, establish target ranges for job–housing balance (preferably 0.5–0.65) in new land supply and urban renewal projects, linking "employment growth–residential provision" with land allocation and performance evaluation to promote short- and medium-distance commuting.
(3) Dynamic peak-hour strategies and an e-bike-friendly network: For congestion corridors characterised by prolonged commuting during the PM peak, public transit operations should prioritise increasing trunk-line bus frequency and improving service reliability, supplemented by feeder minibuses and adequate bicycle parking facilities. These measures help reduce commuters' reliance on buses for trips longer than 4 km and their tendency to shift toward motorised modes when commuting time exceeds one hour. Within the typical commuting radius of 2–6 km, the provision of continuous protected bike lanes, right-

turn waiting areas at intersections, and grade-separated crossings is essential. When combined with a moderate level of land use mix, such infrastructure can strengthen short-distance mode substitution and promote more active commuting choices.

(4) Strengthening walking incentives through 2D compatibility: In communities where land-use compatibility exceeds 0.5, improvements in continuous pedestrian frontages, small-scale corner services, and adequate street lighting can enhance the everyday walking environment. Such interventions help translate morphological compatibility at the spatial level into effective accessibility in residents' daily travel behaviour.

Future research may proceed in the following two directions. First, as this study relies on cross-sectional data and primarily reveals correlations, future work could employ time-series or panel data to explore the causal relationship between land use mix and residents' commute mode choice. Second, due to data limitations, subsequent studies could incorporate street-view imagery to develop more refined measures of 3D land use mix. Nevertheless, the methods applied here are both scientifically grounded and practically meaningful, offering valuable insights for future research. Moreover, further studies should examine the cost-effectiveness of implementing the proposed policy recommendations across different urban contexts, in order to evaluate their financial feasibility and long-term sustainability benefits.

Acknowledgements

The authors would like to express their sincere gratitude to Xu Yuanyuan, Li Xing, Peng Jingjing, and others for their assistance in questionnaire data collection, and to Sun Jiawei for providing valuable comments and suggestions on this manuscript.

Disclosure statement

No potential conflict of interest was reported by the author(s).

Funding

This research was supported by the National Natural Science Foundation of China (Grant No. 52478060) and Key Programme (Grant No. 42330510).

ORCID

Yi Zhu 0009-0006-9034-1862

References

Abdullahi, S., B. Pradhan, S. Mansor, and A. R. M. Shariff. 2015. "GIS-based Modeling for the Spatial Measurement and Evaluation of Mixed Land Use Development for a Compact City." *GIScience & Remote Sensing* 52 (1): 18–39. https://doi.org/10.1080/15481603.2014.993854.

Agency, Xinhua News. 2025. Opinions of the General Office of the Communist Party of China Central Committee and the General Office of the State Council on Continuously Promoting Urban Renewal Initiatives, Accessed 09-25. https://www.gov.cn/zhengce/202505/content_7023880.htm.

Alagbé, A. J., S. Jin, Q. Bao, and W. Guo. 2023. "Estimating Lane Utilization for Variable Approach Lanes Using Explainable Machine Learning." *Transportmetrica B: Transport Dynamics* 11 (1): 2250562. https://doi.org/10.1080/21680566.2023.2250562.

An, R., Z. Tong, B. Tan, Q. Xiong, Y. Luo, Y. Liu, L. Yang, and X. Yang. 2025. "Revealing the Relationship between 2D/3D Built Environment and Jobs-Housing Separation Coupling Nonlinearity and Spatial Nonstationarity." *Journal of Transport Geography* 123: 104112. https://doi.org/10.1016/j.jtrangeo.2025.104112.

Ao, Y., Y. Long, J. Zheng, and H. Bahmani. 2025. "The Influence of Rural Built Environment on residents' Non-Commuting Travel Mode Choices." *Journal of Transport Geography* 128: 104330. https://doi.org/10.1016/j.jtrangeo.2025.104330.

Ashik, F. R., A. I. Z. Sreezon, M. H. Rahman, N. M. Zafri, and S. M. Labib. 2024. "Built Environment Influences Commute Mode Choice in a Global South Megacity Context: Insights from Explainable Machine Learning Approach." *Journal of Transport Geography* 116: 103828. https://doi.org/10.1016/j.jtrangeo.2024.103828.

Ashik, F. R., Rahman, M. Hamidur, N. M. Zafri, A. Antipova, and S. M. Labib. 2024. "Car Ownership, Commute Distance, and Commute Mode Choice in the Dense Megacity of a Developing Country: The Direct and Indirect Role of the Built Environment." *Transportation Research Record* 2678: 19231923–19381938. https://doi.org/10.1177/03611981241253578.

Babahajiani, P., L. Fan, J.-K. Kämäräinen, and M. Gabbouj. 2017. "Urban 3D Segmentation and Modelling from Street View Images and LiDAR Point Clouds." *Machine Vision and Applications* 28 (7): 679–694. https://doi.org/10.1007/s00138-017-0845-3.

Burnell, J. D. 1985. "Industrial Land Use, Externalities, and Residential Location." *Urban Studies* 22 (5): 399–408. https://doi.org/10.1080/00420988520080711.

Cardozo, O., J. C. Daniel, J. García-Palomares, and Gutiérrez. 2012. "Application of Geographically Weighted Regression to the Direct Forecasting of Transit Ridership at Station-Level." *Applied Geography* 34: 548–558. https://doi.org/10.1016/j.apgeog.2012.01.005.

Cervero, R. 1996. "Mixed Land-Uses and Commuting: Evidence from the American Housing Survey." *Transportation Research Part A: Policy and Practice* 30 (5): 361–377. https://doi.org/10.1016/0965-8564(95)00033-x.

Chen, E., Q. Luo, J. Chen, and Y. He. 2023. "Understanding Passenger Travel Choice Behaviours under Train Delays in Urban Rail Transits: A Data-Driven Approach." *Transportmetrica B: Transport Dynamics* 11 (1): 1496–1524. https://doi.org/10.1080/21680566.2023.2226824.

Chen, Z., T. Wu, J. Cao, J. Zhao, S. Li, Z. You, R. Qiao, Z. Wu, and S. Zhou. 2025. "How Street View Shapes Cycling Behaviour during Extreme Heat: A Case Study from Shanghai." *Transportmetrica B: Transport Dynamics* 13 (1): 2537383. https://doi.org/10.1080/21680566.2025.2537383.

Chia, J., and J. Lee. 2020. "Extending Public Transit Accessibility Models to Recognise Transfer Location." *Journal of Transport Geography* 82: 102618. https://doi.org/10.1016/j.jtrangeo.2019.102618.

State Council of the People's Republic of China. 2025. Opinions of the General Office of the Communist Party of China Central Committee and the General Office of the State Council on Continuously Promoting Urban Renewal Initiatives. https://www.gov.cn/zhengce/202505/content_7023880.htm.

Ministry of Natural Resources of the People's Republic of China. 2025. The "Multiple Plans Integration" Territorial Spatial Planning System Has Basically Taken Shape. https://www.gov.cn/lianbo/bumen/202505/content_7024468.htm.

Cui, Y., S. Mishra, and T. F. Welch. 2014. "Land Use Effects on Bicycle Ridership: A Framework for State Planning Agencies." *Journal of Transport Geography* 41: 220–228. https://doi.org/10.1016/j.jtrangeo.2014.10.004.

De Vos, J., L. Cheng, M. Kamruzzaman, and F. Witlox. 2021. "The Indirect Effect of the Built Environment on Travel Mode Choice: A Focus on Recent Movers." *Journal of Transport Geography* 91: 102983. https://doi.org/10.1016/j.jtrangeo.2021.102983.

Ding, C., X. Cao, and P. Næss. 2018. "Applying Gradient Boosting Decision Trees to Examine Non-Linear Effects of the Built Environment on Driving Distance in Oslo." *Transportation Research Part A: Policy and Practice* 110: 107–117. https://doi.org/10.1016/j.tra.2018.02.009.

Dong, L., H. Jiang, W. Li, B. Qiu, H. Wang, and W. Qiu. 2023. "Assessing Impacts of Objective Features and Subjective Perceptions of Street Environment on Running Amount: A Case Study of Boston." *Landscape and Urban Planning* 235: 104756. https://doi.org/10.1016/j.landurbplan.2023.104756.

Dovey, K., and E. Pafka. 2017. "What Is Functional Mix? an Assemblage Approach." *Planning Theory & Practice* 18 (2): 249–267. https://doi.org/10.1080/14649357.2017.1281996.

Evans, S., R. Liddiard, and P. Steadman. 2019. "Modelling a Whole Building Stock: Domestic, Non-Domestic and Mixed Use." *Building Research & Information* 47 (2): 156–172. https://doi.org/10.1080/09613218.2017.1410424.

Gehrke, S. R., and K. J. Clifton. 2016. "Toward a Spatial-Temporal Measure of Land-Use Mix." *Journal of Transport and Land Use* 9 (1): 171–186.

Grant, J. 2002. "Mixed Use in Theory and Practice: Canadian Experience with Implementing a Planning Principle." *Journal of the American Planning Association* 68 (1): 71–84. https://doi.org/10.1080/01944360208977192.

Guo, C., W. Wan, X. Sun, and Y. Jiang. 2025. "Gender-Specific Nonlinear Built Environment Impacts on E-bike Travel Towards Inclusive Sustainability." *Transportmetrica B: Transport Dynamics* 13 (1): 2542418. https://doi.org/10.1080/21680566.2025.2542418.

Gutiérrez, J., O. D. Cardozo, and J. C. García-Palomares. 2011. "Transit Ridership Forecasting at Station Level: An Approach Based on Distance-Decay Weighted Regression." *Journal of Transport Geography* 19 (6): 1081–1092. https://doi.org/10.1016/j.jtrangeo.2011.05.004.

Hawkins, J., and K. Nurul Habib. 2024. "A Framework for Transportation and Land Use Integration as a Parallel Constrained Multiple Discrete-Continuous Extreme Value (PC-MDCEV) Home Production Model." *Transportmetrica B: Transport Dynamics* 12 (1): 2303042. https://doi.org/10.1080/21680566.2024.2303042.

Hendrigan, C., and P. Newman. 2017. "Dense, Mixed-Use, Walkable Urban Precinct to Support Sustainable Transport or Vice Versa? a Model for Consideration from Perth, Western Australia." *International Journal of Sustainable Transportation* 11 (1): 11–19. https://doi.org/10.1080/15568318.2015.1106225.

Jacobs, J. 1993. *The Death and Life of Great American*. New York: Random House.

Jian, W., X. Liu, H. Liu, Y. Hu, and L. Gao. 2023. "The Impacts of the Multiscale Built Environment on Commuting Mode Choice: Spatial Heterogeneity, Moderating Effects, and Implications for Demand Estimation." *Journal of Advanced Transportation* 2023: 1–14. https://doi.org/10.1155/2023/9346631.

Kalogianni, E., P. van Oosterom, E. Dimopoulou, and C. Lemmen. 2020. “3D Land Administration: A Review and a Future Vision in the Context of the Spatial Development Lifecycle.” *ISPRS International Journal of Geo-Information* 9 (2): 107. https://doi.org/10.3390/ijgi9020107.

Kent, J. L., M. Crane, N. Waidyatillake, M. Stevenson, and L. Pearson. 2023. “Urban Form and Physical Activity through Transport: A Review Based on the d-variable Framework.” *Transport Reviews* 43 (4): 726–754. https://doi.org/10.1080/01441647.2023.2165575.

Kong, H., D. Z. Sui, X. Tong, and X. Wang. 2015. “Paths to Mixed-Use Development: A Case Study of Southern Changping in Beijing, China.” *Cities* 44: 94–103. https://doi.org/10.1016/j.cities.2015.01.003.

Krizek, K. J. 2003. “Operationalizing Neighborhood Accessibility for Land Use - Travel Behavior Research and Regional Modeling.” *Journal of Planning Education and Research* 22 (3): 270–287. https://doi.org/10.1177/0739456X02250315.

Labetski, A., S. Vitalis, F. Biljecki, K. Arroyo Ohori, and J. Stoter. 2023. “3D Building Metrics for Urban Morphology.” *International Journal of Geographical Information Science* 37 (1): 36–67. https://doi.org/10.1080/13658816.2022.2103818.

Lee, J., J. Kwak, Y. Oh, and S. Kim. 2023. “Quantifying Incident Impacts and Identifying Influential Features in Urban Traffic Networks.” *Transportmetrica B: Transport Dynamics* 11 (1): 279–300. https://doi.org/10.1080/21680566.2022.2063205.

Litman, T. 2017. Land Use Impacts on Transport: How Land Use Factors Affect Travel Behavior In *Victoria Transport Policy Institute*.

Lu, Y., G. Sun, C. Sarkar, Z. Gou, and Y. Xiao. 2018. “Commuting Mode Choice in a High-Density City: Do Land-Use Density and Diversity Matter in Hong Kong?” *International Journal of Environmental Research and Public Health* 15: 920. https://doi.org/10.3390/ijerph15050920.

Luo, W., and F. Wang. 2003. “Measures of Spatial Accessibility to Health Care in a GIS Environment: Synthesis and a Case Study in the Chicago Region.” *Environment and Planning B: Planning and Design* 30 (6): 865–884. https://doi.org/10.1068/b29120.

Ma, X., J. Yang, C. Ding, J. Liu, and Q. Zhu. 2018. “Joint Analysis of the Commuting Departure Time and Travel Mode Choice: Role of the Built Environment.” *Journal of Advanced Transportation* 2018: 1–13. https://doi.org/10.1155/2018/4540832.

Ma, Y., R. Miao, Z. Chen, B. Zhang, and L. Bao. 2022. “An Interpretable Analytic Framework of the Relationship between Carsharing Station Development Patterns and Built Environment for Sustainable Urban Transportation.” *Journal of Cleaner Production* 377: 134445. https://doi.org/10.1016/j.jclepro.2022.134445.

Manaugh, K., and T. Kreider. 2013. “What Is Mixed Use? Presenting an Interaction Method for Measuring Land Use Mix.” *Journal of Transport and Land Use* 6 (1): 63–72. https://doi.org/10.5198/jtlu.v6i1.291.

Nourinejad, M., and M. Amirgholy. 2022. “Parking Design and Pricing for Regular and Autonomous Vehicles: A Morning Commute Problem.” *Transportmetrica B: Transport Dynamics* 10 (1): 159–183. https://doi.org/10.1080/21680566.2021.1981485.

Palacios, M., and A. El-Geneidy. 2022. “Cumulative Versus Gravity-Based Accessibility Measures: Which One to Use.” *Findings* 32444: 32444.

Raux, C., A. Lamatkhanova, and L. Grassot. 2021. “Does the Built Environment Shape Commuting? The Case of Lyon (France).” *Cybergeo*, 36629. https://doi.org/10.4000/CYBERGEO.36629.

Rith, M., M. Alexis, and J. B. M. Biona. 2019. “Development and Application of a Travel Mode Choice Model and Policy Implications for Home-To-Work Commuters Toward Reduction of Car Trips in Metro Manila.” *Asian transport studies* 5: 862862–873873. https://doi.org/10.11175/EASTSATS.5.862.

Shen, L., Y. Long, L. Tian, S. Wang, and M. Wang. 2023. “The Impact of Built Environment on the Commuting Distance of Middle/Low-income Tenant Workers in Mega Cities Based on Nonlinear Analysis in Machine Learning.” *Urban Rail Transit* 9 (4): 294–309. https://doi.org/10.1007/s40864-023-00202-4.

Song, Y., L. Merlin, and D. Rodriguez. 2013. “Comparing Measures of Urban Land Use Mix.” *Computers, Environment and Urban Systems* 42: 1–13. https://doi.org/10.1016/j.compenvurbsys.2013.08.001.

Sun, B., and C. Yin. 2019. “Impacts of a Multi-Scale Built Environment and Its Corresponding Moderating Effects on Commute Duration in China.” *Urban Studies* 57 (10): 2115–2130. https://doi.org/10.1177/0042098019871145.

Sun, B., A. Ermagun, and B. Dan. 2017. “Built Environmental Impacts on Commuting Mode Choice and Distance: Evidence from Shanghai.” *Transportation Research Part D-transport and Environment* 52: 441441–453453. https://doi.org/10.1016/J.TRD.2016.06.001.

Tian, L., Y. Liang, and B. Zhang. 2017. “Measuring Residential and Industrial Land Use Mix in the Peri-Urban Areas of China.” *Land Use Policy* 69: 427–438. https://doi.org/10.1016/j.landusepol.2017.09.036.

UN-Habitat. 2013. Planning and Design for Sustainable Urban Mobility: Global Report on Human Settlements 2013 In Nairobi.

Vale, D. S., M. Saraiva, and M. Pereira. 2016. “Active Accessibility: a Review of Operational Measures of Walking and Cycling Accessibility.” *Journal of Transport and Land Use* 9 (1): 209–235. https://doi.org/10.5198/jtlu.2015.593.

van Wee, B., and S. Handy. 2016. “Key Research Themes on Urban Space, Scale, and Sustainable Urban Mobility.” *International Journal of Sustainable Transportation* 10(1): 18–24. https://doi.org/10.1080/15568318.2013.820998.

Wang, X., C. Shao, C. Yin, and C. Dong. 2020. “Exploring the Effects of the Built Environment on Commuting Mode Choice in Neighborhoods Near Public Transit Stations: Evidence from China.” *Transportation Planning and Technology* 44: 111111–127127. https://doi.org/10.1080/03081060.2020.1851453.

Wang, Z., E. Yang Yang, Y. Yao, Z. Zhu, and Rao. 2021. "An Analysis of Commute Mode Choice Behavior Considering the Impacts of Built Environment in Beijing." *Transportation Letters* 14: 733733–739739. https://doi.org/10.1080/19427867.2021.1938908.

Wei, J., Z. Kan, Z. Liu, Z. Wang, and Y. Chen. 2025. "Exploring Spatio-Temporal Variations in Nonlinear Correlations between the Built Environment and Metro-Bike Travel: Evidence from Beijing." *Transportmetrica B: Transport Dynamics* 13 (1): 2541282. https://doi.org/10.1080/21680566.2025.2541282.

Wu, C.-D., S.-C. C. Lung, and J.-F. Jan. 2013. "Development of a 3-D Urbanization Index Using Digital Terrain Models for Surface Urban Heat Island Effects." *ISPRS Journal of Photogrammetry and Remote Sensing* 81: 1–11. https://doi.org/10.1016/j.isprsjprs.2013.03.009.

Wu, L., X. Cheng, C. Kang, D. Zhu, Z. Huang, and Y. Liu. 2020. "A Framework for Mixed-Use Decomposition Based on Temporal Activity Signatures Extracted from Big Geo-Data." *International Journal of Digital Earth* 13(6): 708–726. https://doi.org/10.1080/17538947.2018.1556353.

Xia, C., J. Zhou, Y. Wang, J. Zhang, S. Li, B. Li, F. Xue, D. Tian, X. Zheng, and J. Zhao. 2025. "How Is the Urban Built Environment Associated with Commuting Carbon Emissions during the COVID-19 Pandemic: A Case Study in Hangzhou, China." *Cities* 165: 106100. https://doi.org/10.1016/j.cities.2025.106100.

Xu, X., D. Ding, and X. Liu. 2024. "A Three-Dimensional Future Land Use Simulation (FLUS-3D) Model for Simulating the 3D Urban Dynamics under the Shared Socio-Economic Pathways." *Landscape and Urban Planning* 250: 105135. https://doi.org/10.1016/j.landurbplan.2024.105135.

Yang, Y., H. Chung, and J. S. Kim. 2021. "Local or Neighborhood? Examining the Relationship between Traffic Accidents and Land Use Using a Gradient Boosting Machine Learning Method: The Case of Suzhou Industrial Park, China." *Journal of Advanced Transportation* 2021: 1. 8246575. https://doi.org/10.1155/2021/8246575.

Yang, Y., C. Wang, W. Liu, and P. Zhou. 2018. "Understanding the Determinants of Travel Mode Choice of Residents and Its Carbon Mitigation Potential." *Energy Policy* 115: 486–493. https://doi.org/10.1016/j.enpol.2018.01.033.

Yang, L., Y. Ao, J. Ke, Y. Lu, and Y. Liang. 2021. "To Walk or Not to Walk? Examining Non-Linear Effects of Streetscape Greenery on Walking Propensity of Older Adults." *Journal of Transport Geography* 94: 103099. https://doi.org/10.1016/j.jtrangeo.2021.103099.

Yue, Y., Y. Zhuang, A. G. Yeh, J.-Y. Xie, C.-L. Ma, and Q.-Q. Li. 2016. "Measurements of POI-based Mixed Use and Their Relationships with Neighbourhood Vibrancy." *International Journal of Geographical Information Science* 31: 1–18. https://doi.org/10.1080/13658816.2016.1220561.

Zhang, M., and P. Zhao. 2017. "The Impact of Land-Use Mix on residents' Travel Energy Consumption: New Evidence from Beijing." *Transportation Research Part D: Transport and Environment* 57: 224–236. https://doi.org/10.1016/j.trd.2017.09.020.

Zhang, Y., H. Zhao, and Y. Long. 2025. "CMAB: a Multi-Attribute Building Dataset of China." *Scientific Data* 12 (1): 430. https://doi.org/10.1038/s41597-025-04730-5.

Zhang, C., L. Li, R. Liu, and L. Ahmad. 2025. "Transportation Corridors and Land Use Interaction: a Multi-Disciplinary Critical Review." *Transportmetrica B: Transport Dynamics* 13 (1): 2561865. https://doi.org/10.1080/21680566.2025.2561865.

Zhang, Y., C. Yu, C. Yang, W. Dong, and W. Li. 2025. "Spend More but Get Less: Unravelling the Causes of Bus Ridership Decline Using a Data-Driven Machine Learning Approach." *Transportmetrica B: Transport Dynamics* 13 (1): 2438246. https://doi.org/10.1080/21680566.2024.2438246.

Zhang, W., Y. Dai, Z. Hu, R. Cao, C. Yu, and W. Li. 2025. "Rethinking Dynamic Interactions between Commuting Public Transit Modal Share and Land Use Patterns." *Transportmetrica B: Transport Dynamics* 13 (1): 2514477. https://doi.org/10.1080/21680566.2025.2514477.

Zhao, X., N. Xia, and M. Li. 2023. "3-D Multi-Aspect Mix Degree Index: a Method for Measuring Land Use Mix at Street Block Level." Computers, Environment and Urban Systems 104: 102005. https://doi.org/10.1016/j.compenvurbsys.2023.102005.

Zhou, X., A. G. Yeh, Y. Yue, and W. Li. 2022. "Residential-Employment Mixed Use and Jobs-Housing Balance: a Case Study of Shenzhen, China." *Land Use Policy* 119: 106201. https://doi.org/10.1016/j.landusepol.2022.106201.

Zhu, P., K. Wang, S.-N. Ho, and X. Tan. 2023. "How Is Commute Mode Choice Related to Built Environment in a High-Density Urban Context?" *Cities* 134: 104180. https://doi.org/10.1016/j.cities.2022.104180.

Zhuo, Y., H. Zheng, C. Wu, Z. Xu, G. Li, and Z. Yu. 2019. "Compatibility Mix Degree Index: a Novel Measure to Characterize Urban Land Use Mix Pattern." *Computers, Environment and Urban Systems* 75: 49–60. https://doi.org/10.1016/j.compenvurbsys.2019.01.005.

Zou, L., Z. Wang, R. Guo, and L. Zhao. 2025. "Decoding Urban Transportation: Trade-Offs in Mode Choices Using Big Data." *Transportation Research Part D: Transport and Environment* 143: 104756. https://doi.org/10.1016/j.trd.2025.104756.